Manual for

A Power Flow Programme

(Version 1.0)

Prepared by

Dr. K.N. Shubhanga

Mr. Chandra S.R.

Department of Electrical Engineering

NITK, Surathkal

Srinivasnagar, Mangalore - 575025

KARNATAKA, INDIA

Contents

List of Figures

List of Tables

Chapter 1

Load Flow Studies: An Introduction

1.1 Introduction:

One of the most common computational procedures used in power system analysis is the load flow calculation. Based on the assumed load demands, generation levels and transmission network configuration, the load flow calculations provides the complete steady-state information about the system such as the overall voltage profile (bus voltage magnitudes and bus angles), power flows in the branches, line currents, line losses, and other related variables for a given set of specified conditions. Such a steady-state snap-shot analysis provides the basic data for various studies involving planning, design, and operation of power systems. Application areas of load flow studies are listed below [1, 2]:

1. System planning: This includes some of following tasks:
   (a) Transmission planning: It involves design, analysis, sizing of conductors, transformers, reactors, shunt capacitors, and future planning of transmission circuits.
   (b) Interchange studies to identify line over-loadings, violation of bus voltages limits, inappropriately large bus phase angles etc.
   (c) Generation adequacy studies and generation planning.
   (d) Cost to benefit analysis of system additions.
2. System operation and control: Some of the important studies carried out include
   (a) Economic dispatch of the generating stations (i.e.,calculating the power levels at each generating unit such that the system is operated most economically).
   (b) Contingency analysis (analysis of outages and other forced operating conditions).

(c) Studies that ensure power pool coordination.

(d) Generation dispatch and load demand control.

(e) Operation tasks related to day to day and week to week operation of the system.

(f) Studies pertaining to scheduling of phase shifters, tap changing transformers, reactive power controlling devices etc.

(g) Studies related to settings of protective gears.

3. The load flow results provides the basic data for various other studies, for example: short circuit analysis, small-signal and transient stability studies, security constrained stability analysis: as optimal power flow routine, long-term small-signal voltage stability studies: continuation power flow programme, etc.

1.2 Load flow Problem Formulation:

The load flow analysis of a power system involves the following steps:

1. Formulation of a suitable mathematical model for the network.
2. Specifications of power and voltage constraints at various buses of the network.
3. Numerical solution of the power flow equations subject to the above constraints.

The load flow calculation is a network solution problem. The necessary equations can be established by using either the bus or loop frame-of-reference [3]. Due to the inherent advantages such as simplicity of data preparation and ease of network representation and computation (exploitation of sparsity), the bus frame-of-reference is normally used for formulation of load flow problem. The equation describing the performance of the network of a power system using the bus frame-of-reference in admittance form is given by

$$\underline{I} = Y_{BUS} \ \ \underline{V} \tag{1.1}$$

where

$\underline{I}$ is the vector of total positive sequence currents injected into the network nodes.

$\underline{V}$ is the vector of total positive sequence voltages at the network nodes.

Y_{BUS} is the network admittance matrix.

If either $\underline{I}$ or $\underline{V}$ were known, the solution for the unknown quantities could be obtained by the solution of *linear algebraic* equations represented by (1.1). Partly because of tradition and partly because of the physical characteristics of generation and load, the

terminal conditions at each bus are normally described in terms of a vector of net injected active and reactive power ($\underline{P}$ and $\underline{Q}$). The injected bus current $\underline{I}$ is calculated as:

$$\underline{I} = \frac{(\underline{P} + j\underline{Q})^*}{\underline{V}^*} \tag{1.2}$$

Combining (1.1) and (1.2) yields

$$\left[\frac{(\underline{P} + j\underline{Q})^*}{\underline{V}^*}\right] = Y_{BUS} \;\; \underline{V} \tag{1.3}$$

Note that the above equation is *nonlinear* and can not be readily solved by closed form matrix techniques. Because of this, load flow solutions are obtained by employing numerical techniques involving iterative procedures.

Let P_p and Q_p denote the net injected real and reactive power at bus p as shown in Figure 1.1.

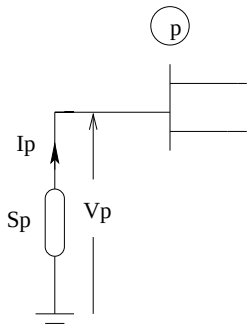

Figure 1.1: Representation of a typical bus p in load flow studies.

Then, the complex power *injected* at bus p is given by

$$S_p = P_p + jQ_p = V_p I_p^*$$

where Q_p represents inductive reactive power and a negative Q_p represents capacitive reactive power.

From (1.1), the injected current at bus p, I_p can be calculated as

$$I_p = \sum_{q=1}^{n} Y_{pq} V_q, \quad p = 1, 2, ..., n \tag{1.4}$$

where n represents the number of buses in a system and $V_q = |V_q| \angle \delta_q$

Using (1.4) we can write an expression for apparent power S_p at bus p as

$$S_p = V_p \sum_{q=1}^{n} Y_{pq}^* V_q^* \tag{1.5}$$

In the above equation, equating the real and imaginary parts on both sides we get the active and reactive power balance equations as follows, which constitute the power-flow equations.

$$P_p = \text{Re}\left[V_p \sum_{p=1}^{n} Y_{pq}^* V_q^*\right] \tag{1.6}$$

$$Q_p = \text{Im}\left[V_p \sum_{q=1}^{n} Y_{pq}^* V_q^*\right] \tag{1.7}$$

for $p = 1, 2, \ldots, n$

Note that the above set constitutes $2n$ number of nonlinear equations in $6n$ variables with 6 variables at each bus p: bus voltage magnitude $|V_p|$, bus voltage angle δ_p, active power generation P_{Gp}, reactive power generation Q_{Gp}, active power load demand P_{Lp}, reactive power load demand Q_{Lp}. Normally, the generation and load power at a bus are combined to give net injected bus powers, (P_p and Q_p), resulting in 4 variables at each bus. Thus, in load flow problem $2n$ nonlinear equations in $4n$ variables need to be solved. From this, it is clear that it is not possible to obtain a solution for any unknown variables unless we reduce the number of "unknowns" to $2n$ which is equal to the number of connecting equations. In other words, at each bus two of the four variables needs to be a priori specified and the remaining two variables are required to be calculated using the two power balance equations available at that bus. This has lead to the general practice of identification of different types of buses in the network.

1.2.1 Types of Buses:

To enable a priori fixation of some of the variables, the 6 variables at each bus are classified as follows [1, 4]:

1. Demand variables : The demand variables P_{Lp} and Q_{Lp}, can be specified from the knowledge of customer load demand.

2. Generation (or control) variables: The generation variables P_{Gp} and Q_{Gp}, can be specified using the scheduled generation data.

3. State variables: The variables such as voltage magnitude $|V_p|$ and bus angle δ_p completely define the state of a system. These variables are normally treated as

state (or unknown) variables.

Based on this classification, the buses in a system are categorized into 3 types as follows:

1. Load buses (PQ-buses): A load bus is any bus that does not have generation. Here, real power and reactive powers are specified, because for loads, one generally specifies the real power demand, P_{Lp} and the reactive power demand, Q_{Lp}. In some cases, such a bus need not have a load, it may simply be an interconnection point for two or more lines. Those buses are also treated as load buses with $P_{Lp} = Q_{Lp} = 0$.

2. Generator buses (PV-buses): A generator bus is usually called a voltage controlled or PV-bus. Here, real power generation, P_{Gp} and voltage magnitude, $|V_p|$ are normally specified. At such buses voltage magnitude is held constant at a specified value by adjusting the reactive power output of the generator. Based on its capability, maximum and minimum limits on reactive power generation (Q_{Gmax} and Q_{Gmin}) are specified at PV-buses. Certain PV-buses without real power generation may have voltage control capability, such buses are also designated as voltage-controlled buses at which the real power generation is set to zero. A generator bus could also have load connected to it. Based on whether load is present or not at a PV-bus, for the purpose of ease of handling, a PV-bus is further categorized as follows:

   (a) Simple PV-bus : These are buses in which there is no load connected.

   (b) PV-bus with loads : In addition to normal PV- bus specification, loads are also connected at these buses.

3. Swing bus: This is also known as a *reference* bus or *slack bus*. Swing bus is a special type of generator bus that is needed by the solution processes. This requirement comes from the fact that in load flow analysis, the losses in the system cannot be determined unless the converged solution is obtained. This slack in the power balance is accounted in the reference bus generation. Therefore in a power system,

$$\begin{pmatrix} \text{Sum of complex} \\ \text{power of generators} \end{pmatrix} = \begin{pmatrix} \text{Sum of complex} \\ \text{power of loads} \end{pmatrix} + \begin{pmatrix} \text{Total (complex) power} \\ \text{loss in transmission lines} \end{pmatrix}$$

   This model assumes that only the slack bus generates the necessary real and reactive power required for overcoming all system losses. Hence, for the slack bus, the magnitude and phase angle of bus voltage are specified and real and reactive power generations are obtained at the end of the load flow solution. The voltage angle of the slack bus serves as reference for the angles of all other bus voltages.

   A swing bus could also have load connected to it. Based on whether load is present or not swing bus is further categorized into:

(a) Swing bus without load

(b) Swing bus with load

Thus, in a n bus system, there will be one slack bus and there may be m PV-buses and rest of the buses are designated as PQ-buses. The load flow problem formulation results in $2n$ nonlinear algebraic equations in $4n$ variables. Of these $4n$ variables, 2 variables are specified for the slack bus, $2m$ variables are specified for PV-buses and $2(n-m-1)$ variables are specified for PQ-buses. These specifications make $4n-(2+2m+2(n-m-1)) = 2n$ variables to be determined from the load analysis. However, in load flow problem, the nonlinear equations are solved only for $2n-m-2$ unknown variables (voltage magnitudes and bus angles). The remaining $(m+2)$ unknown variables (such as P_{Gs}, Q_{Gs} at slack bus and Q_{Gp} at m PV-buses) are computed. In the solution of nonlinear equations, normally the unknown voltage magnitudes are initialized to 1.0 p.u. and angles are initialized to 0^o. In some cases, the unknown bus voltage vector is initialized to the specified slack bus voltage, which is referred to as flat voltage start [4].
NOTE:

1. The following convention is followed with respect to apparent powers. The apparent power drawn by the load is $S_{Lp} = P_{Lp} + jQ_{Lp}$. Where Q_{Lp} denotes inductive load and a negative Q_{Lp} represents capacitive load.

2. The apparent power injected by the generator is $S_{Gp} = P_{Gp} + jQ_{Gp}$. Where Q_{Gp} represents inductive reactive power and a negative Q_{Gp} represents capacitive reactive power.

1.2.2 Handling of Bus Types in Load Flow Problem:

In load flow study, a separate strategy is followed to handle different types of buses. In the following lines the procedure of handling PV-buses and slack bus is explained:

1.2.2.1 Handling of PV-Buses:

Ii is known that by controlling the the reactive power generation at PV-bus, the voltage magnitude at the PV-bus is maintained at the specified value. If limits on reactive power generation is specified at PV-buses, the checking of Q-limits are carried out in the following manner:

1. While checking for Q-limit specifications at a Simple PV-bus, the computed reactive power $(= Q_p)$ is considered.

2. While checking for Q-limits at a PV-bus with load, the net reactive power generation (Q_{Gp}) is considered. This Q_{Gp} is equal to the sum of reactive power load Q_{Lp} at that bus and the computed reactive power Q_p, (i.e, $Q_{Gp} = Q_{Lp} + Q_p$).

If any Q-limit violation is detected, a PV-bus is handled in any one of the following ways [5]-[7]:

1. Bus-type switching : In any iteration, if Q-limits are violated at a PV-bus, then it is switched to PQ-type with the reactive generation set at the limiting value. In any consequent iteration if Q-limits are satisfied at such a bus, then that bus is reverted back to PV-type with the original bus voltage specification. This is referred to as back-off. Thus, handling of PV-buses in load flow analysis by a way of bus switching calls for repeated adjustments of number of unknowns.

2. Adjusting the specified voltage at PV-buses: In any iteration, if Q-limits are violated at a PV-bus, then the specified voltage at the violated PV-bus is adjusted in such a way that it remains as PV-bus and meets the Q constraints. This procedure avoids the readjustment of number unknowns.

In bus-type switching, it is important to consider the time at which the Q-limits are enforced at PV-buses in the solution process as it may effect the convergence characteristics of an algorithm. If not handled properly, such an enforcement may slow down the convergence or even cause the solution to oscillate or even diverge [9]. The main parameters used for the starting criteria are:

1. Iteration count [8]: In this case, the bus-type switching at each PV-buses is delayed until the second or later iterations.

2. Bus power mismatches [9]: In this case, the bus-type switching at each PV-buses is delayed until the reactive power mismatch is sufficiently small (i.e., load flow solution is moderately converged).

1.2.2.2 Handling of Slack Bus:

The real and reactive power generations at slack bus are calculated from the converged load flow results as follows:

$$S_{Gs} = S_s = V_s \sum_{q=1}^{n} Y_{sq}^* V_q^* \tag{1.8}$$

If any load is present at slack bus, then the real and reactive components of load are simply added to the computed values to obtain the net power generation at slack bus.

$$S_{Gs} = (P_{Gs} + jQ_{Gs}) = S_s + (P_{Ls} + jQ_{Ls}) \tag{1.9}$$

1.2.3 Load Flow Solution Methods:

Load flow studies for power system analysis are based on static network models assuming sinusoidal steady state. As a result the equations are algebraic in form rather than differential. The usual power flow problem formulation does not consider time variation of loads, generation, or network configuration. The load flow problem formulation is nonlinear in nature even for a linear transmission network since power specification is employed which is a product of voltage and current. Additional nonlinearities arise due to specification and use of complex voltages and currents. Also, there are transmission component nonlinearities, which may be considered (such as tap changing transformers in which the tap is adjusted to hold a given bus voltage magnitude fixed). Thus, load flow problem generally involves the simultaneous solution of many nonlinear algebraic equations. Since it is not feasible to obtain solution in a closed form directly for nonlinear system of equations, numerical techniques are normally employed involving iterative procedure. Some of the popularly used methods are fixed-point (Gauss) methods and Newton based methods.

The earliest algorithms were based on the Gauss-Seidel methods, which are very simple and reliable. However, it takes extremely large computation times when applied to systems of increasing size due to its poor convergence characteristics [1, 3, 10]. To overcome the drawbacks in the these methods, a new method called "Newton's method" was introduced in early sixties [8]. This method basically comprises the repeated solution of a large set of linear equations which are obtained by linearizing the load flow equations. Newton's methods have very powerful convergence properties, but with poor computational efficiency and also it requires large storage memory. To improve the computational speed and storage requirements of the Newton Raphson method, B. Stoot and O. Alasc have developed 'fast decoupled load flow method' in early 1970's [7] which is a modification of the Newton method.

Chapter 2

Newton-Raphson Method

2.1 Introduction To Newton-Raphson Method:

The application of Newton's method to load flow problem is essentially the n-dimensional generalization of the well known Newton-Raphson method [6, 11] for the solution of a nonlinear equation in one variable. Taylor's series expansion for a function of two or more variables is the basis for the Newton-Raphson method of solving the load-flow problem [12]. Let the following represent n nonlinear equations in n unknowns :

$$\begin{aligned} f_1(x_1, x_2, \cdots, x_n) &= b_1 \\ f_2(x_1, x_2, \cdots, x_n) &= b_2 \\ \cdots\cdots\cdots\cdots\cdots &\cdots \cdots \\ f_n(x_1, x_2, \cdots, x_n) &= b_n \end{aligned} \tag{2.1}$$

If the iterations start with an initial estimate of $x_1^0, x_2^0, \cdots, x_n^0$ for n unknowns and if $\Delta x_1, \Delta x_2, \cdots, \Delta x_n$ are the corrections necessary to the estimates so that the equations are exactly satisfied, we have

$$\begin{aligned} f_1(x_1^0 + \Delta x_1, x_2^0 + \Delta x_2, \cdots, x_n^0 + \Delta x_n) &= b_1 \\ f_2(x_1^0 + \Delta x_1, x_2^0 + \Delta x_2, \cdots, x_n^0 + \Delta x_n) &= b_2 \\ \cdots\cdots\cdots\cdots\cdots\cdots\cdots\cdots\cdots &\cdots \cdots \\ f_n(x_1^0 + \Delta x_1, x_2^0 + \Delta x_2, \cdots, x_n^0 + \Delta x_n) &= b_n \end{aligned} \tag{2.2}$$

Each of the above equations can be expanded using Taylor's theorem. The expanded

form of the i^{th} equation is

$$f_i(x_1^0+\Delta x_1,\ldots,x_n^0+\Delta x_n) = \left\{\begin{array}{l} f_1(x_1^0,x_2^0,\cdots,x_n^0)+\left(\dfrac{\partial f_i}{\partial x_1}\right)\Delta x_1+\left(\dfrac{\partial f_i}{\partial x_2}\right)\Delta x_2 \\ +\ldots+\left(\dfrac{\partial f_i}{\partial x_n}\right)\Delta x_n+\text{terms with} \\ \text{higher powers of } \Delta x_1,\ldots,\Delta x_n \end{array}\right\} = b_i$$

The terms of higher powers can be neglected, if our initial estimate is close to the true solution. The resulting linear set of equations in matrix form is

$$\begin{bmatrix} b_1-f_1(x_1^0,x_2^0,\cdots,x_n^0) \\ b_2-f_1(x_1^0,x_2^0,\cdots,x_n^0) \\ \cdots\cdots\cdots\cdots\cdots\cdots \\ b_n-f_1(x_1^0,x_2^0,\cdots,x_n^0) \end{bmatrix} = \begin{bmatrix} \left(\dfrac{\partial f_1}{\partial x_1}\right)_0 & \left(\dfrac{\partial f_1}{\partial x_2}\right)_0 & \cdots & \left(\dfrac{\partial f_1}{\partial x_n}\right)_0 \\ \left(\dfrac{\partial f_2}{\partial x_1}\right)_0 & \left(\dfrac{\partial f_2}{\partial x_2}\right)_0 & \cdots & \left(\dfrac{\partial f_2}{\partial x_n}\right)_0 \\ \cdots & \cdots & \cdots & \cdots \\ \left(\dfrac{\partial f_n}{\partial x_1}\right)_0 & \left(\dfrac{\partial f_n}{\partial x_2}\right)_0 & \cdots & \left(\dfrac{\partial f_n}{\partial x_n}\right)_0 \end{bmatrix}^o \begin{bmatrix} \Delta x_1 \\ \Delta x_2 \\ \cdots \\ \Delta x_n \end{bmatrix} \quad (2.3)$$

or in general,

$$\Delta \underline{F} = J\ \Delta \underline{x}$$

where J is referred to as the **Jacobian**. If the estimates $x_1^0,\cdots,x_n^0$ were exact, then $\Delta\underline{F}$ and $\Delta\underline{x}$ would be zero. However, as $x_1^0,\cdots,x_n^0$ are only estimates, the errors $\Delta\underline{F}$ are finite. The above equation provides a linearized relationship between the errors $\Delta\underline{F}$ and the corrections $\Delta\underline{x}$ through the Jacobian of the simultaneous equations. A solution for $\Delta\underline{x}$ can be obtained by applying any suitable method for the solution of a set of linear equations. An updated value of x can be calculated as

$$x_i^1 = x_i^0 + \Delta x_i$$

The process is repeated until the errors ΔF_i are lower than a specified tolerance. The Jacobian has to be recalculated at each step.

Newton's method possesses quadratic convergence characteristics, a feature not shared by other methods. Its drawback is that the initial guess used should be close to the solution for the process to converge. For power systems this is not a serious drawback since a good initial guess is generally available from experience [8].

2.2 Application of the Newton-Raphson Method to Load Flow Solution:

In general, there are three types of approaches available in literature for solving load flow equations using Newton's method [10]. Those are:

1. Rectangular power-mismatch version: This version uses the real and imaginary parts of the bus voltages (i.e., rectangular co-ordinate system $e_i + jf_i$) as variables.
2. Polar power-mismatch version: This version uses the magnitudes and angles of the bus voltages (i.e., polar co-ordinate system ($|V|\angle\delta$) as variables.
3. Current-mismatch version: In this version, rectangular and polar coordinate version are constructed using the real and imaginary parts of the complex current expression.

Polar power-mismatch version is widely used version of the Newton's method, because of its more reliability and accuracy over rectangular power-mismatch version [10]. So in this report, polar power-mismatch version is considered [6, 11]. In this version we denote

$$\begin{aligned} Y_{pq} &= G_{pq} + jB_{pq} \\ V_p &= |V_p|\angle\delta_p = |V_p|(\cos\angle\delta_p + j\sin\angle\delta_p) \\ V_q &= |V_q|\angle\delta_q = |V_q|(\cos\angle\delta_q + j\sin\angle\delta_q) \end{aligned} \tag{2.4}$$

Using (2.4) in (1.5), the complex power injected at bus p can be represented as

$$P_p + jQ_p = |V_p|\angle\delta_p \sum_{q=1}^{n}((G_{pq} + jB_{pq})|V_q|\angle\delta_q)^* \tag{2.5}$$

Expanding (2.5) and equating real and imaginary parts on both sides, we get

$$P_p = |V_p|\sum_{q=1}^{n}((G_{pq}\cos\delta_{pq} + B_{pq}\sin\delta_{pq)})|V_q|) \tag{2.6}$$

$$Q_p = |V_p|\sum_{q=1}^{n}((G_{pq}\sin\delta_{pq} - B_{pq}\cos\delta_{pq)})|V_q|) \tag{2.7}$$

where $p = 1, 2, \ldots, n$ and $\delta_{pq} = \delta_p - \delta_q$

From the above, it can be seen that P_p and Q_p at each bus are functions of voltage

magnitude $|V|$ and angle δ at all buses and the load flow equations are formulated as:

$$\begin{aligned} P_1(\delta_1, \cdots, \delta_n, |V_1|, \cdots, |V_n|) &= P_1^{sp} \\ &\cdots\cdots\cdots\cdots\cdots\cdots\cdots \\ P_n(\delta_1, \cdots, \delta_n, |V_1|, \cdots, |V_n|) &= P_n^{sp} \\ Q_1(\delta_1, \cdots, \delta_n, |V_1|, \cdots, |V_n|) &= Q_1^{sp} \\ &\cdots\cdots\cdots\cdots\cdots\cdots\cdots \\ Q_n(\delta_1, \cdots, \delta_n, |V_1|, \cdots, |V_n|) &= Q_n^{sp} \end{aligned} \tag{2.8}$$

Note that the above equation is similar to (2.1). The RHS terms denote the power specifications at each bus.

Computation of bus power mismatches:

Having specified real power generation P_{Gp}, and real power load P_{Lp} at bus p, the net specified real power injected into the network at bus p is computed as

$$P_p^{sp} = P_{Gp} - P_{Lp}$$

Similarly, having specified reactive power generation Q_{Gp}, and reactive power load Q_{Lp} at bus p, the net specified reactive power injected into the network at bus p is computed as

$$Q_p^{sp} = Q_{Gp} - Q_{Lp}$$

NOTE:

1. The following convention is followed with respect to apparent powers. The apparent power drawn by the load is $S_{Lp} = P_{Lp} + jQ_{Lp}$. Where Q_{Lp} denotes inductive load. And a negative Q_{Lp} represents capacitive load.

2. The apparent power injected by the generator is $S_{Gp} = P_{Gp} + jQ_{Gp}$. Where Q_{Gp} represents inductive reactive power. And a negative Q_{Gp} represents capacitive reactive power.

Following the general procedure described earlier for the application of the Newton's method, we have

$$\begin{bmatrix} P_1^{sp} - P_1(\delta_1^0, \cdots, \delta_n^0, |V_1^0|, \cdots, |V_n^0|) \\ \cdots\cdots\cdots\cdots\cdots\cdots\cdots\cdots \\ P_n^{sp} - P_n(\delta_1^0, \cdots, \delta_n^0, |V_1^0|, \cdots, |V_n^0|) \\ Q_1^{sp} - Q_1(\delta_1^0, \cdots, \delta_n^0, |V_1^0|, \cdots, |V_n^0|) \\ \cdots\cdots\cdots\cdots\cdots\cdots\cdots\cdots \\ Q_n^{sp} - Q_n(\delta_1^0, \cdots, \delta_n^0, |V_1^0|, \cdots, |V_n^0|) \end{bmatrix}^0 = \begin{bmatrix} \frac{\partial P_1}{\partial \delta_1} & \cdots & \frac{\partial P_1}{\partial \delta_n} & \frac{\partial P_1}{\partial |V_1|} & \cdots & \frac{\partial P_1}{\partial |V_n|} \\ \cdots & \cdots & \cdots & \cdots & \cdots & \cdots \\ \frac{\partial P_n}{\partial \delta_1} & \cdots & \frac{\partial P_n}{\partial \delta_n} & \frac{\partial P_n}{\partial |V_1|} & \cdots & \frac{\partial P_n}{\partial |V_n|} \\ \frac{\partial Q_1}{\partial \delta_1} & \cdots & \frac{\partial Q_1}{\partial \delta_n} & \frac{\partial Q_1}{\partial |V_1|} & \cdots & \frac{\partial Q_1}{\partial |V_n|} \\ \cdots & \cdots & \cdots & \cdots & \cdots & \cdots \\ \frac{\partial Q_n}{\partial \delta_1} & \cdots & \frac{\partial Q_n}{\partial \delta_n} & \frac{\partial Q_n}{\partial |V_1|} & \cdots & \frac{\partial Q_n}{\partial |V_n|} \end{bmatrix}^0 \begin{bmatrix} \Delta\delta_1 \\ \cdots \\ \Delta\delta_n \\ \Delta|V_1| \\ \cdots \\ \Delta|V_n| \end{bmatrix}^0 \quad (2.9)$$

The above equation is similar to (2.3). The LHS vector represents the power mismatch at each buses $[\Delta\underline{P}, \Delta\underline{Q}]^T$. The real power mismatch at bus p, pertaining to the first iteration (k=0), ΔP_p^0 is calculated as

$$\Delta P_p^0 = P_p^{sp} - P_p^0 \quad (2.10)$$

Using (2.6), the above equation is re-written as

$$\Delta P_p^0 = P_p^{sp} - |V_p^0| \sum_{q=1}^{n} ((G_{pq} \cos\delta_{pq}^0 + B_{pq} \sin\delta_{pq}^0)|V_q^0|) \quad (2.11)$$
$$p = 1, 2, \ldots, n \quad \text{and} \quad p \neq \text{slack bus}$$

Similarly, reactive power mismatch at bus p, pertaining to the first iteration (k=0), ΔQ_p^0 is calculated as

$$\Delta Q_p^0 = Q_p^{sp} - Q_p^0 \quad (2.12)$$

Using (2.7), the above equation is re-written as

$$\Delta Q_p^0 = Q_p^{sp} - |V_p^0| \sum_{q=1}^{n} ((G_{pq} \sin\delta_{pq}^0 - B_{pq} \cos\delta_{pq}^0)|V_q^0|) \quad (2.13)$$
$$p = 1, 2, \ldots, n; \quad p \neq \text{slack bus}, \quad p \neq \text{PV-bus}$$

To bring-in symmetry in the elements of the Jacobian, the linearized load flow equation given in (2.9) is modified (for the k^{th} iteration) as follows:

$$\begin{bmatrix} \Delta\underline{P} \\ \Delta\underline{Q} \end{bmatrix}^{(k-1)} = \begin{bmatrix} H & N \\ M & L \end{bmatrix}^{(k-1)} \begin{bmatrix} \Delta\delta \\ \frac{\Delta|\underline{V}|}{|\underline{V}|} \end{bmatrix}^{(k-1)} \tag{2.14}$$

where the submatrices elements are defined as

$$[H]_{(n-1)\times(n-1)} = \frac{\partial\underline{P}}{\partial\underline{\delta}} \qquad [N]_{(n-1)\times(n-1-m)} = \frac{\partial\underline{P}}{\frac{\partial|\underline{V}|}{|\underline{V}|}}$$

$$[M]_{(n-1-m)\times(n-1)} = \frac{\partial\underline{Q}}{\partial\delta} \quad [L]_{(n-1-m)\times(n-1-m)} = \frac{\partial\underline{Q}}{\frac{\partial|\underline{V}|}{|\underline{V}|}}$$

NOTE:

1. In H submatrix the row and column corresponding to slack bus are not present.
2. In L submatrix the rows and columns corresponding to slack bus and PV-buses are not present.
3. In N submatrix the row and column corresponding to slack bus and columns corresponding to PV-buses are not present.
4. In M submatrix the row and column corresponding to slack bus and rows corresponding to PV-buses are not present.

2.2.1 Calculation of Elements of Submatrices:

Each submatrices (H, N, M, L) will have its own diagonal and off-diagonal elements. When $p = q$: it represents the diagonal elements and $p \neq q$ represents the off-diagonal elements. The elements H, N, M, and L matrices are calculated as follows.

1. Calculation of H submatrix:

   (a) Off-diagonal element H_{pq} is given by, $H_{pq} = \dfrac{\partial P_p}{\partial \delta_q}$

   Rewriting (2.6) we,have

$$P_p = |V_p| \sum_{q=1}^{n} ((G_{pq}\cos\delta_{pq} + B_{pq}\sin\delta_{pq}))|V_q|) \tag{2.15}$$

   where p = 1,2,. . . ,n

And differentiating P_p with respect to δ_q, we have

$$\frac{\partial P_p}{\partial \delta_q} = \frac{\partial}{\partial \delta_q}|V_p| \left\{ \begin{array}{c} (G_{p1}\cos(\delta_p - \delta_1) + B_{p1}\sin(\delta_p - \delta_1))|V_1| + \ldots \\ (G_{pq}\cos(\delta_p - \delta_q) + B_{pq}\sin(\delta_p - \delta_q))|V_q| + \ldots \\ (G_{pn}\cos(\delta_p - \delta_n) + B_{pn}\sin(\delta_p - \delta_n))|V_n| \end{array} \right\}$$

where p = 1,2,. . . ,n

Simplifying above equation, we get

$$H_{pq} = |V_p||V_q|(G_{pq}\sin\delta_{pq} - B_{pq}\cos\delta_{pq)}) \tag{2.16}$$

(b) Diagonal elements H_{pp} is given by, $H_{pp} = \dfrac{\partial P_p}{\partial \delta_p}$

Differentiating (2.6) with respect to δ_p, we,have

$$\frac{\partial P_p}{\partial \delta_p} = \frac{\partial}{\partial \delta_p}|V_p| \left\{ \begin{array}{c} (G_{p1}\cos(\delta_p - \delta_1) + B_{p1}\sin(\delta_p - \delta_1))|V_1| + \ldots \\ (G_{pq}\cos(\delta_p - \delta_q) + B_{pq}\sin(\delta_p - \delta_q))|V_q| + \ldots \\ (G_{pn}\cos(\delta_p - \delta_n) + B_{pn}\sin(\delta_p - \delta_n))|V_n| \end{array} \right\}$$

where p = 1,2,. . . ,n

Simplifying the above equation, we get

$$H_{pp} = |V_p| \sum_{\substack{q=1 \\ q \neq p}}^{n} -G_{pq}\sin(\delta_p - \delta_q) + B_{pq}\cos(\delta_p - \delta_q))|V_q| \tag{2.17}$$

Using (2.7), the above expression can be simplified as

$$H_{pp} = -Q_p - B_{pp}|V_p|^2 \tag{2.18}$$

Following the procedure detailed above we can obtain the expressions for the elements of other submatrices, M, N and L as follows:

2. Calculation of M submatrix:

(a) Off diagonal element M_{pq} is given by:

$$M_{pq} = \frac{\partial Q_p}{\partial \delta_q} = -|V_p||V_q|(G_{pq}\cos\delta_{pq} + B_{pq}\sin\delta_{pq)}) \tag{2.19}$$

(b) Diagonal element M_{pp} is given by:

$$M_{pp} = \frac{\partial Q_p}{\partial \delta_p} = P_p - G_{pp}|V_p|^2 \tag{2.20}$$

3. Calculation of N submatrix:

(a) Off-diagonal element N_{pq} is given by:

$$N_{pq} = \frac{\partial P_p}{\frac{\partial |V_q|}{|V_q|}} = |V_p||V_q|(G_{pq}\cos\theta_{pq} + B_{pq}\sin\theta_{pq)}) \tag{2.21}$$

(b) Diagonal elements N_{pp} is given by:

$$N_{pp} = \frac{\partial P_p}{\frac{\partial |V_p|}{|V_p|}} = P_p + G_{pp}|V_p|^2 \tag{2.22}$$

4. Calculation of L submatrix:

(a) Off diagonal element L_{pq} is given by:

$$L_{pq} = \frac{\partial Q_p}{\frac{\partial |V_q|}{|V_q|}} = |V_p||V_q|(G_{pq}\sin\delta_{pq} - B_{pq}\cos\delta_{pq)}) \tag{2.23}$$

(b) Diagonal element L_{pp} is given by:

$$L_{pp} = \frac{\partial Q_p}{\frac{\partial |V_p|}{|V_p|}} = Q_p - B_{pp}|V_p|^2 \tag{2.24}$$

Using (2.18), we can write that

$$L_{pp} = -H_{pp} - 2B_{pp}|V_p|^2 \tag{2.25}$$

From above expressions it can be seen that $H_{pq} = L_{pq}$ and $N_{pq} = -M_{pq}$. This is due to the fact that the voltage magnitude increment $\Delta|V|$ at a PQ-bus is divided by $|V|$.
NOTE:

1. The real and reactive power mismatch vectors are updated along with the Jacobian elements at the beginning of solving (2.14). The maximum value of mismatch vector, $[\Delta\underline{P}^0, \Delta\underline{Q}^0]^T$ will be considerable at the beginning of power flow solution depending on the closeness of the initial guess $(|\underline{V}|^0, \underline{\delta}^0)$ to the final solution. If the iterative

solution process tends to converge, then the maximum value of the mismatch vector tends to zero. Normally, the solution process is terminated if the maximum value of the power mismatch falls below a tolerance factor ϵ (which is set to 0.001 or 0.0001), i.e. if

$$max|[\Delta \underline{P}, \Delta \underline{Q}]^T| \ \leq \ \epsilon$$

then the load flow solution is said to be converged.

2. In each of the $(k-1)^{th}$ iterative step, a solution of the linearized system of equation is carried out. Here, k denotes the iterative count and is set equal to 1.

3. In $(k-1)^{th}$ iterative step, the mismatch vector $[\Delta \underline{P}^{(k-1)}, \Delta \underline{Q}^{(k-1)}]^T$ and the Jacobian elements are calculated using $|\underline{V}|^{(k-1)}$ and $\underline{\delta}^{(k-1)}$ values.

4. In $(k-1)^{th}$ iterative step, the correction vector $[\Delta \underline{\delta}^{(k-1)}, \frac{\Delta |\underline{V}|^{(k-1)}}{|\underline{V}|^{(k-1)}}]$ is obtained by solving the linear system of equations. Using this correction vector the voltage magnitude and angle are updated at bus p as follows:

$$\delta_p^k = \delta_p^{(k-1)} + \Delta \delta_p^{(k-1)} \tag{2.26}$$

$$\begin{aligned} |V_p|^k &= |V_p|^{(k-1)} + \frac{\Delta |V_p|^{(k-1)}}{|V_p|^{(k-1)}} |V_p|^{(k-1)} \\ \text{or} & \\ |V_p|^k &= |V_p|^{(k-1)} \left(1 + \frac{\Delta |V_p|^{(k-1)}}{|V_p|^{(k-1)}}\right) \end{aligned} \tag{2.27}$$

2.3 Newton-Raphson Algorithm:

In this section the steps involved in the N-R method of load flow analysis is presented. The algorithm has been implemented for the following two different cases:

1. PV-buses without Q-limits specifications.

2. PV-buses with Q-limits specifications.

2.3.1 PV-buses Without Q-limits Specifications:

The implementation steps are depicted in flow chart shown in Figure 2.1. The 'Q-bit' is set equal to 0 for for this case.

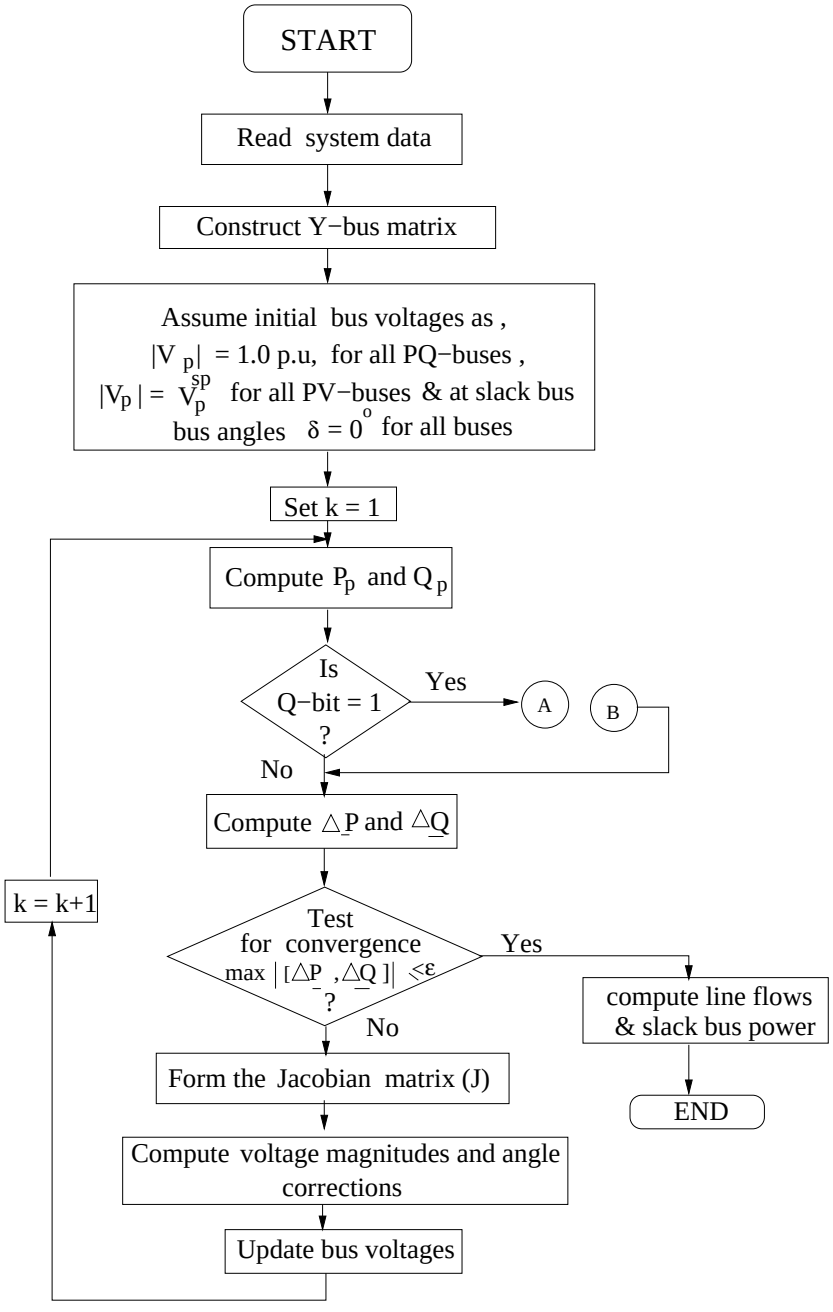

Figure 2.1: Flow chart for the implementation of Newton-Raphson method

2.3.1.1 Load Flow Study Example:

The single line diagram of a 4 bus, 2 machine power system is shown in Figure 2.2. The system details have been adopted from Example 9.2 [11]. Base used is 100 MVA.

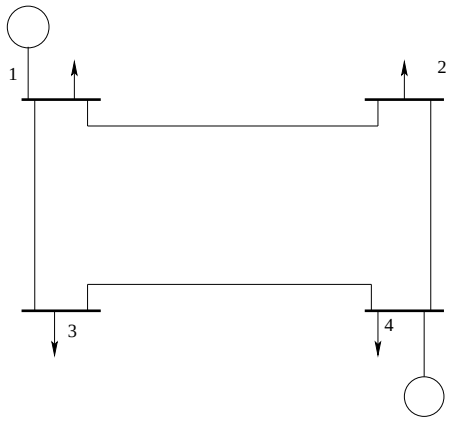

Figure 2.2: One line diagram for load flow example.

The bus data and line data are as follows:

From	To	r (pu)	x (pu)	y(total) (pu)
1	2	0.01008	0.05040	0.1025
1	3	0.00744	0.03720	0.0775
2	4	0.00744	0.03720	0.0775
3	4	0.01272	0.06360	0.1275

Table 2.1: Line data for the example.

Bus No.p	Generation		Load		$\|V_p\|$ (pu)	Type
	P_{Gp} (MW)	Q_{Gp} (MVAr)	P_{Lp} (MW)	Q_{Lp} (MVAr)		
1	-	-	50	30.99	1.00	Slack-bus
2	0	0	170	105.35	-	PQ-bus
3	0	0	200	123.94	-	PQ-bus
4	318	-	80	49.58	1.02	PV-bus

Table 2.2: Bus data for the example.

NOTE: The data files have been provided in the folder `4_bus_example`.

1. Constructing the bus admittance matrix Y_{BUS}, using bus admittance algorithm. we have,

$$\begin{bmatrix} 8.9852 - j44.8360 & -3.8156 + j19.0781 & -5.1696 + j25.8478 & 0 \\ -3.8156 + j19.0781 & 8.9852 - j44.8360 & 0 & -5.1696 + j25.8478 \\ -5.1696 + j25.8478 & 0 & 8.1933 - j40.8638 & -3.0237 + j15.1185 \\ 0 & -5.1696 + j25.8478 & -3.0237 + j15.1185 & 8.1933 - j40.8638 \end{bmatrix}$$

2. Assume $|V_1| = 1.0$ pu, $|V_2| = 1.0$ pu and $|V_3| = 1.0$ pu. And $\delta_2, \delta_3, \delta_4 = 0$. And the convergence factor $\epsilon = 0.001$

Iteration 1:

1. The specified bus powers and calculated bus powers (using the initial bus voltages) are :

Bus No.p	P_p^{sp}	P_p	Q_p^{sp}	Q_p
2	-1.7	-0.1034	-1.0535	-0.6070
3	-2.0	-0.0605	-1.2394	-0.4049
4	2.38	0.1671	-	0.7291

2. Using the computed bus power mismatches and the Jacobian elements we have (as per (2.14)),

$$\begin{array}{c} 2 \\ 3 \\ 4 \\ 2 \\ 3 \end{array} \left[\begin{array}{ccc|cc} 45.4429 & 0 & -26.3648 & 8.8818 & 0 \\ 0 & 41.2687 & -15.4209 & 0 & 8.1328 \\ -26.3648 & -15.4209 & 41.7857 & -5.2730 & -3.0842 \\ \hline -9.0886 & 0 & 5.2730 & 44.2290 & 0 \\ 0 & -8.2537 & 3.0842 & 0 & 40.4590 \end{array}\right] \left[\begin{array}{c} \Delta\delta_2 \\ \Delta\delta_3 \\ \Delta\delta_4 \\ \hline \frac{\Delta|V_2|}{|V_2|} \\ \frac{\Delta|V_3|}{|V_3|} \end{array}\right] = \left[\begin{array}{c} -1.5966 \\ -1.9395 \\ 2.2129 \\ \hline -0.4465 \\ -0.8345 \end{array}\right] \quad (2.28)$$

3. Solving the above equation, we get the corrections to the voltage magnitudes and angles as:

Bus No.p	$\Delta\delta_p$ (deg)	$\Delta\|V_p\|$ (pu)
2	-0.9309	-0.0166
3	-1.7879	-0.0290
4	1.5438	

4. At the end of the first iteration, the set of updated bus voltages are:

Bus No.p	1	2	3	4
δ_p (deg)	0	-0.9309	-1.7879	1.5438
$\|V_p\|$ (per unit)	1.00	0.9834	0.9710	1.02

Iteration 2:

1. The specified bus powers and the bus powers calculated (using the updated bus voltages at the end of 1^{st} iteration) are:

Bus No.p	P_p^{sp}	P_p	Q_p^{sp}	Q_p
2	-1.7	-1.6677	-1.0535	-1.0193
3	-2.0	-1.9355	-1.2394	-1.1774
4	2.38	2.3441		

2. Using the computed bus power mismatches and the Jacobian elements we have (as per (2.14)),

$$\begin{array}{c} 2 \\ 3 \\ 4 \\ \hline 2 \\ 3 \end{array} \left[\begin{array}{ccc|cc} 44.37499 & 0 & -25.6778 & 7.0208 & 0 \\ 0 & 39.7018 & -14.7736 & 0 & 5.7887 \\ -26.1256 & -15.1217 & 41.2473 & -4.0609 & -2.1193 \\ \hline -10.3562 & 0 & 6.2998 & 42.3363 & 0 \\ 0 & -9.6597 & 3.8597 & 0 & 37.3470 \end{array}\right] \left[\begin{array}{c} \Delta\delta_2 \\ \Delta\delta_3 \\ \Delta\delta_4 \\ \hline \frac{\Delta|V_2|}{|V_2|} \\ \frac{\Delta|V_3|}{|V_3|} \end{array}\right] = \left[\begin{array}{c} -0.0323 \\ -0.0645 \\ 0.0359 \\ \hline -0.0342 \\ -0.0620 \end{array}\right]$$

3. Solving the above equation, we get the corrections to the voltage magnitudes and angles as:

Bus No.p	$\Delta\delta_p$ (deg)	$\Delta\|V_p\|$ (pu)
2	-0.0451	-0.0009
3	-0.00841	-0.0019
4	0.0207	

At the end of 2^{nd} iteration: The specified and the bus powers calculated (using the updated bus voltages at the end of 2^{nd} iteration) are:

Bus No.p	P_p^{sp}	P_p	ΔP_p	Q_p^{sp}	Q_p	ΔQ_p
2	-1.7	-1.7000	0.00	-1.0535	-1.0535	0.00
3	-2.0	-1.9999	0.0001	-1.2394	-1.2392	0.0002
4	2.38	2.38	0.0	-	-	-

From above table, it is observed that the calculated bus power mismatches falls below ϵ. The converged results are shown in Table 2.3 :

Bus No. p	$\lvert V_p\rvert$ (pu)	δ_p (deg)	P_{Gp} (pu)	Q_{Gp} (pu)	P_{Lp} (pu)	Q_{Lp} (pu)
1	1.000000	0.000000	1.867948	1.144877	0.500000	0.309900
2	0.982422	-0.976035	0.000000	0.000000	1.700000	1.053500
3	0.969010	-1.871975	0.000000	0.000000	2.000000	1.239400
4	1.020000	1.523147	3.180000	1.814193	0.800000	0.495800

Table 2.3: Converged load flow results: without Q-limits

2.3.2 PV-buses With Q-limits Specifications:

In N-R method, PV-buses are handled by a way of bus-type switching and iteration count is used as the starting criteria since it is easy to implement and is well suited for the N-R method because of its unified nature of its solution for $[\Delta\underline{\delta}, \Delta|\underline{V}|]^T$. The implementation logic is shown in Figure 2.3. The 'Q-bit' set to 1 in Figure 2.1.

2.3.2.1 Load Flow Study Example:

For the test system shown in Figure 2.2, the maximum reactive power limit at PV-bus 4 is $Q_{Gmax} = 0.4$ and the minimum reactive power limit is $Q_{Gmin} = 0$. The load flow results are given as follows. Note that in the results given, the *starting criteria is not accounted* just to demonstrate the intermediate steps. This done by setting `start_cri` = 0 in `jacob_form.m`

Iteration 1:

1. The specified bus powers and the bus powers calculated (using the initial bus voltages) are :

Bus No.p	P_p^{sp}	P_p	Q_p^{sp}	Q_p
2	-1.7	-0.1034	-1.0535	-0.6070
3	-2.0	-0.0605	-1.2394	-0.4049
4	2.38	0.1671	-	0.7291

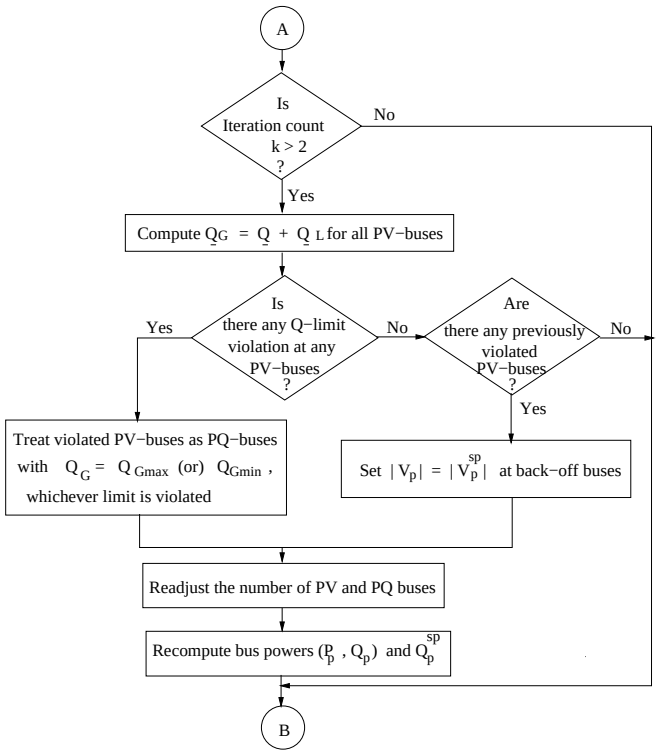

Figure 2.3: Flow chart for the standard bus-type switching logic.

2. Here, at bus 4 a real load of $P_{L4} = 0.8$ pu. and a reactive load of $Q_{L4} = 0.4958$ pu. is present. While checking the Q-limits at PV-bus, the required reactive power generation is calculated as: $Q_{G4} = Q_4 + Q_{L4} = 0.7291 + 0.4958 = 1.2249$ pu. Note that $Q_{G4} > Q_{Gmax}$. Therefore, this bus is treated as a PQ-bus with $Q_{G4} = 0.4$ pu. Further, $Q_4^{sp} = Q_{G4} - Q_{L4} = 0.4$ - 0.4958 = -0.0958 pu. and $\Delta Q_4 = Q_4^{sp} - Q_4 =$ -0.0958 - 0.7291 = -0.8249 pu. The initial bus voltage magnitude is 1.02 pu.

3. Using the computed bus power mismatches and the Jacobian elements we have (as per (2.14))

$$
\begin{array}{c}
2 \\ 3 \\ 4 \\ \hline 2 \\ 3 \\ 4
\end{array}
\left[\begin{array}{ccc|ccc}
45.4429 & 0 & -26.3648 & 8.8818 & 0 & -5.2730 \\
0 & 41.2687 & -15.4209 & 0 & 8.1328 & -3.0842 \\
-26.3648 & -15.4209 & 41.7857 & -5.2730 & -3.0842 & 8.6914 \\ \hline
-9.0886 & 0 & 5.2730 & 44.2290 & 0 & -26.3648 \\
0 & -8.2537 & 3.0842 & 0 & 40.4590 & -15.4209 \\
5.2730 & 3.0842 & -8.3571 & -26.3648 & -15.4209 & 43.2438
\end{array}\right]
\left[\begin{array}{c}
\Delta\delta_2 \\ \Delta\delta_3 \\ \Delta\delta_4 \\ \hline \frac{\Delta|V_2|}{|V_2|} \\ \frac{\Delta|V_3|}{|V_3|} \\ \frac{\Delta|V_3|}{|V_3|}
\end{array}\right]
=
\left[\begin{array}{c}
-1.5966 \\ -1.9395 \\ 2.2129 \\ \hline -0.4465 \\ -0.8345 \\ -0.8249
\end{array}\right]
$$

The above equation is identical to (2.28) except for an additional row and column pertaining to bus 4.

4. Solving the above equation, we get the corrections to the voltage magnitudes and angles as:

Bus No.p	$\Delta\delta_p$ (deg)	$\Delta\|V_p\|$ (pu)
2	-5216	-0.0512
3	-1.5240	-0.0511
4	2.2467	-0.0591

5. At the end of the first iteration the updated bus voltages are:

Bus No. p	1	2	3	4
δ_p (deg)	0	-0.5216	-1.5240	2.2467
$\|V_p\|$ (per unit)	1.00	0.9488	0.9489	0.9609

At the end of 3^{rd} iteration: The specified bus powers and the bus powers calculated (using the updated bus voltages at the end of 3^{rd} iteration) are:

Bus No.p	P_p^{sp}	P_p	ΔP_p	Q_p^{sp}	Q_p	ΔQ_p
2	-1.7	-1.7000	0.000	-1.0535	-1.0535	0.000
3	-2.0	-1.9999	0.000	-1.2394	-1.2394	0.000
4	2.38	2.38	0.000	-0.0958	-0.0958	0.000

From above table, it is observed that the calculated bus power mismatches fall below ϵ. The converged results are shown in Table 2.4 :

Bus No.p	$\|V_p\|$ (pu)	δ_p (deg)	P_{Gp} (pu)	Q_{Gp} (pu)	P_{Lp} (pu)	Q_{Lp} (pu)
1	1.000000	0.000000	1.884566	2.667856	0.500000	0.309900
2	0.941383	-0.533208	0.000000	0.000000	1.700000	1.053500
3	0.942312	-1.631389	0.000000	0.000000	2.000000	1.239400
4	0.951521	2.636509	3.180000	0.400001	0.800000	0.495800

Table 2.4: Converged Load flow results: accounting Q-limits at bus 4.

NOTE:

- It is observed that with the enforcement of Q-limits specifications at PV-buses causes the Newton's method to take more number of iterations.

- When Q-limits at PV-buses are handled by a way of bus-type switching it requires resizing of jacobian whenever there is any new Q-limit violations and back-offs in each iterative step. In MATLAB, this involves the solution of a linear system of equations in the usual manner (see Appendix).
- Since Q-limit has been imposed at bus 4, the bus voltage is no longer held at 1.02 pu. which is the specified value.

2.3.3 A Case Study to Demonstrate the Effect of Point of Enforcement of Q-limits Based on Iteration Count:

Case studies are carried out on IEEE 30 and 300 bus systems [13], to demonstrate the effect of point of enforcement of Q-limits using 'iteration count' (k) as the starting criteria. The results are presented in the following lines:

Type of system	No of iterations			
	At starting	$k > 1$	$k > 2$	$k > 3$
IEEE 30 bus system	6	3	3	2
IEEE 300 bus system	NC	NC	8	4

Table 2.5: Effect of iteration count as the starting criteria (NR-method).

From Table 2.5, it is observed that the enforcement of Q-limits at starting causes divergence in the IEEE 300-bus system and also it makes the solution to take more number of iterations in the IEEE 30-bus system. For value of $k > 2$, the IEEE 300-bus system converges. For $k > 3$, no Q-limits are enforced and hence the solution converges without accounting Q-limits at PV-buses for the IEEE 30-bus system. However, for $k > 3$, the solution converges within 4 iterations for the IEEE 300-bus system. In this report a value of $k > 2$ has been used as the starting criteria for all systems. This done by setting `start_cri` $= 2$ in `jacob_form.m`.

2.3.4 Convergence Results for the IEEE Systems:

The results obtained using the IEEE test systems [13, 14] are presented in Tables 2.6 and 2.7. In the tables NC denotes failure to converge. Base used is 100 MVA. The approximate execution time is obtained in a P4 computer (3 GHz, 512 MB DDR 400 MHz memory, 910 GL chipset) and it also includes the time for report generation.

IEEE system	Iterations	Execution time (s)
14-bus	2	0.032
30-bus	2	0.032
57-bus	3	0.047
118-bus	3	0.094
145-bus	NC	-
162-bus	3	0.156
300-bus	4	0.281

Table 2.6: IEEE test system results without accounting Q-limits at PV-buses (NR).

IEEE system	Iterations	Execution time (s)
14-bus	2	0.047
30-bus	3	0.062
57-bus	3	0.062
118-bus	NC	-
300-bus	8	0.481

Table 2.7: IEEE test system results accounting Q-limits at PV-buses (NR).

Chapter 3

Case Studies with A Test System: NR method

3.1 The IEEE 14-bus System

The single line diagram of the IEEE 14-bus system is shown in Figure 3.1. The system details are adopted from [13].

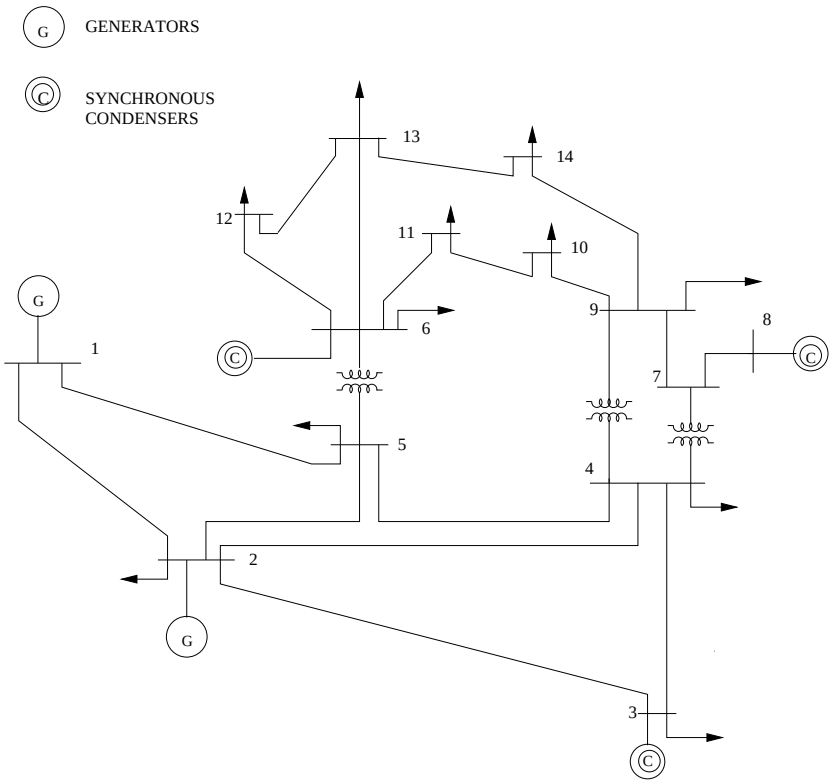

Figure 3.1: The IEEE 14-bus system

3.2 Newton-Raphson method

To run the load flow programme using Newton-Raphson method, the file required is: `loadflow.m`. This file in turn calls the following `.m` files:

1. `ybus_form.m`: It constructs the Y_{BUS}
2. `jacob_form.m`: It constructs the Jacobian matrix and performs the solution of load flow linearized equation till the solution is converged.
3. `powerflow.m`: It calculates the line flows and line losses.
4. `lfl_result.m`: It constructs the result files: `lfl.dat` and `report.dat`.

The above files require the following data files:

1. `busno.dat` : System details- number of lines, buses, transformers, etc.
2. `nt.dat` : Transmission line and transformer data.
3. `pvpq.dat` : Generation data and load data.
4. `shunt.dat` : Shunt data.
5. `Qlim_data.dat` : Reactive power generation limits data at PV-buses.

On successful run, it generates two output files: `lfl.dat` and `report.dat`. The converged loadflow results are available in `lfl.dat`.

3.2.1 Format of Data Files

In the following lines the format of each of the data file has been given using the IEEE 14-bus system data:
System details:

```
File name: busno.dat
------------------------------------------------------------------------
1       -----> Slack bus number.
0.001   -----> Loadflow convergence tolerance.
14      -----> Number of buses in the system.
17      -----> Number of lines.
3       -----> Number of transformers.
4       -----> Number of PV buses = (Number of generators - 1).
1       -----> To account Q-limits set this bit 1, otherwise 0. (Q-bit)
```

```
11      -----> Number of load buses (including loads at PV and slack buses).
1       -----> Number of shunts.
1.06    -----> Slack bus voltage magnitude.
------------------------------------------------------------------------
```

Network data:

File name: nt.dat

From	To	R	X	y (total)/Tap ratio	Remarks
1	2	0.01938	0.05917	0.0528	---> Line 1
1	5	0.05403	0.22304	0.0492	---> Line 2
2	3	0.04699	0.19797	0.0438	---> Line 3
2	4	0.05811	0.17632	0.034	---> Line 4
2	5	0.05695	0.17388	0.034	---> Line 5
3	4	0.06701	0.17103	0.0128	---> Line 6
4	5	0.01335	0.04211	0.00	---> Line 7
7	8	0.0	0.17615	0.0	---> Line 8
7	9	0.0	0.11001	0.0	---> Line 9
9	10	0.03181	0.08450	0.0	---> Line 11
6	11	0.09498	0.19890	0.0	---> Line 11
6	12	0.12291	0.25581	0.0	---> Line 12
6	13	0.06615	0.13027	0.0	---> Line 13
9	14	0.12711	0.27038	0.0	---> Line 14
10	11	0.08205	0.19207	0.0	---> Line 15
12	13	0.22092	0.19988	0.0	---> Line 16
13	14	0.17093	0.34802	0.0	---> Line 17
4	7	0.0	0.20912	0.978 ---> Transformer data starts here.	
4	9	0.0	0.55618	0.969	
5	6	0.0	0.25202	0.932	

Generation and load data:

File name: pvpq.dat

Bus No.	Vg/PL0	Pg0/QL0	Remarks
2	1.045	0.4	---->Generator buses other than the slack bus
3	1.010	0	are specified as PV buses.
6	1.070	0	
8	1.090	0	
2	0.217	0.127	----> Load data starts here (including loads at
3	0.942	0.19	and slack buses).
6	0.112	0.075	
4	0.478	-0.039	
5	0.076	0.016	
9	0.295	0.166	
10	0.090	0.058	
11	0.035	0.018	
12	0.061	0.016	
13	0.135	0.058	
14	0.149	0.050	

Shunt admittances:

File name: shunt.dat

Bus No.	G	B
9	0	0.19

NOTE: The file `Qlim_data.dat` will be used if 'Q-bit'= 1.
Q-Limits data at PV-buses.

File name: Qlim_data.dat

PV Bus No.	Qmin	Qmax
2	-0.4	0.5
3	0.0	0.4
6	-0.60	0.24
8	-0.60	0.24

The system has taken 2 iterations to reach convergence and the converged load flow results accounting Q-limits at PV-buses are as follows:

File name: lfl.dat

Bus No	VbO	thetaO	PGO	QGO	PLO	QLO
1	1.060000	0.000000	2.323125	-0.165537	0.000000	0.000000
2	1.045000	-4.980701	0.400000	0.435235	0.217000	0.127000
3	1.010000	-12.721706	0.000000	0.250445	0.942000	0.190000
4	1.017716	-10.310331	0.000000	0.000000	0.478000	-0.039000
5	1.019556	-8.771159	0.000000	0.000000	0.076000	0.016000
6	1.070000	-14.216144	0.000000	0.126609	0.112000	0.075000
7	1.061581	-13.357956	0.000000	0.000000	0.000000	0.000000
8	1.090000	-13.357956	0.000000	0.175853	0.000000	0.000000
9	1.055992	-14.938240	0.000000	0.000000	0.295000	0.166000
10	1.051039	-15.096276	0.000000	0.000000	0.090000	0.058000
11	1.056948	-14.787257	0.000000	0.000000	0.035000	0.018000
12	1.055207	-15.071036	0.000000	0.000000	0.061000	0.016000
13	1.050404	-15.152100	0.000000	0.000000	0.135000	0.058000
14	1.035576	-16.032367	0.000000	0.000000	0.149000	0.050000

The partial content of file `report.dat` is shown below. The expressions used for the calculation of line flows and the system losses are given in Appendix.

```
Line flows:
```

		Line flows				Line flows	
From	To	P-flow	Q-flow	From	To	P-flow	Q-flow
1	2	1.5683	-0.2039	2	1	-1.5253	0.2765
1	5	0.7549	0.0384	5	1	-0.7273	0.0224
2	3	0.7322	0.0356	3	2	-0.7090	0.0160
2	4	0.5612	-0.0157	4	2	-0.5444	0.0304
2	5	0.4150	0.0118	5	2	-0.4060	-0.0205
3	4	-0.2329	0.0445	4	3	0.2366	-0.0481
4	5	-0.6117	0.1583	5	4	0.6168	-0.1421
7	8	0.0000	-0.1713	8	7	0.0000	0.1759
7	9	0.2810	0.0578	9	7	-0.2810	-0.0498
9	10	0.0522	0.0423	10	9	-0.0520	-0.0420
6	11	0.0736	0.0354	11	6	-0.0730	-0.0342
6	12	0.0778	0.0250	12	6	-0.0771	-0.0235
6	13	0.1775	0.0720	13	6	-0.1754	-0.0678
9	14	0.0942	0.0362	14	9	-0.0931	-0.0337
10	11	-0.0380	-0.0160	11	10	0.0382	0.0163
12	13	0.0161	0.0075	13	12	-0.0161	-0.0075
13	14	0.0565	0.0174	14	13	-0.0560	-0.0162
4	7	0.2809	-0.0969	7	4	-0.2809	0.1139
4	9	0.1609	-0.0043	9	4	-0.1609	0.0174
5	6	0.4407	0.1249	6	5	-0.4407	-0.0807

```
Total real power losses in the system =  0.133859
Total reactive power losses in the system =  0.089733
```

Chapter 4

Fast Decoupled Load Flow Method

4.1 Introduction to FDLF Method:

FDLF method is characterized by a decoupling of the linearized loadflow equations with constant load flow matrices. This method is an alternative to the Newton method provided the following three conditions are met:

1. The voltages are around their nominal values.
2. The angle difference across the lines is small.
3. The $\frac{X}{R}$ ratios are relatively large for all branches.

Fast decoupled load flow method is an approximate version of the Newton-Raphson Method. The principle underlying the decoupled approach is based on the following two standard observations in normal situations corresponding to a stable operating state of a power system:

1. Change in the bus angle δ at a bus predominantly affects the real power flow in the transmission lines and leaves the reactive power flow relatively unchanged.
2. Change in the voltage magnitude $|V_p|$ at a bus primarily affects the flow of reactive power in the transmission lines and leaves the flow of real power relatively unchanged.

The development of FDLF method [7] from the Newton's method has been explained in the following sections.

4.2 Development of FDLF Equations:

Following the general procedure described earlier for the application of the Newton-Raphson method in section 2.2, we have

$$\begin{bmatrix} \triangle \underline{P} \\ \triangle \underline{Q} \end{bmatrix} = \begin{bmatrix} \dfrac{\partial \underline{P}}{\partial \underline{\delta}} & \dfrac{\partial \underline{P}}{\partial |\underline{V}|} \\ \dfrac{\partial \underline{Q}}{\partial \underline{\delta}} & \dfrac{\partial \underline{Q}}{\partial |\underline{V}|} \end{bmatrix} \begin{bmatrix} \triangle \underline{\delta} \\ \triangle |\underline{V}| \end{bmatrix} \tag{4.1}$$

The first observation indicated above, essentially states that $\frac{\partial P}{\partial \delta}$ is much larger than $\frac{\partial Q}{\partial \delta}$ and the second observation states that $\frac{\partial Q}{\partial |V|}$ is much larger than $\frac{\partial P}{\partial |V|}$. Employing these approximations in the Jacobian of (4.1), we get,

$$\begin{bmatrix} \triangle \underline{P} \\ \triangle \underline{Q} \end{bmatrix} = \begin{bmatrix} \dfrac{\partial \underline{P}}{\partial \underline{\delta}} & 0 \\ 0 & \dfrac{\partial \underline{Q}}{\partial |\underline{V}|} \end{bmatrix} \begin{bmatrix} \triangle \underline{\delta} \\ \triangle |\underline{V}| \end{bmatrix} \tag{4.2}$$

Expanding (4.2) we have

$$\begin{bmatrix} \dfrac{\partial P_1}{\partial \delta_1} & \cdots & \dfrac{\partial P_1}{\partial \delta_n} \\ \vdots & \vdots & \vdots \\ \dfrac{\partial P_n}{\partial \delta_1} & \cdots & \dfrac{\partial P_n}{\partial \delta_n} \end{bmatrix} \begin{bmatrix} \triangle \delta_1 \\ \vdots \\ \triangle \delta_n \end{bmatrix} = \begin{bmatrix} \triangle P_1 \\ \vdots \\ \triangle P_n \end{bmatrix} \tag{4.3}$$

$$\begin{bmatrix} |V_1| \dfrac{\partial Q_1}{\partial |V_1|} & \cdots & |V_n| \dfrac{\partial Q_1}{\partial |V_n|} \\ \vdots & \vdots & \vdots \\ |V_1| \dfrac{\partial Q_n}{\partial |V_1|} & \cdots & |V_n| \dfrac{\partial Q_n}{\partial |V_n|} \end{bmatrix} \begin{bmatrix} \dfrac{\triangle V_1}{|V_1|} \\ \vdots \\ \dfrac{\triangle V_n}{|V_n|} \end{bmatrix} = \begin{bmatrix} \triangle Q_1 \\ \vdots \\ \triangle Q_n \end{bmatrix} \tag{4.4}$$

The above equations are decoupled in the sense that the voltage-angle corrections $\triangle \underline{\delta}$ are calculated using only real power mismatches $\triangle \underline{P}$, while the voltage magnitude corrections are calculated using only $\triangle \underline{Q}$ mismatches. However the coefficient matrices of (4.3) and (4.4) are still interdependent. Because of this interdependency, it would still require the evaluation and factoring of the two coefficient matrices at each iteration. To avoid such computations, the elements of the coefficient matrices are simplified as follows [11]:

Modified off-diagonal elements: Rewriting the expression for off-diagonal elements of H and L submatrices, from (2.16) and (2.23), we have

$$\frac{\partial P_p}{\partial \delta_q} = \frac{\partial Q_p}{\frac{\partial |V_q|}{|V_q|}} = |V_p||V_q|(G_{pq}\sin\delta_{pq} - B_{pq}\cos\delta_{pq}) \tag{4.5}$$

Using the following assumptions in the above expression,

1. The angular differences $(\delta_p - \delta_q)$ between typical buses of the system are usually so small that
$$\cos(\delta_p - \delta_q) = 1; \quad \sin(\delta_p - \delta_q) = (\delta_p - \delta_q) \tag{4.6}$$

2. The susceptance B_{pq} is many times larger than the conductance G_{pq} so that
$$G_{pq}\sin(\delta_p - \delta_q) << B_{pq}\cos(\delta_p - \delta_q) \tag{4.7}$$

we have,

$$\frac{\partial P_p}{\partial \delta_q} = \frac{\partial Q_p}{\frac{\partial |V_q|}{|V_q|}} = -|V_p||V_q|B_{pq} \tag{4.8}$$

Modified diagonal elements: Rewriting the expression for diagonal element of H submatrix, from (2.18), we have

$$\frac{\partial P_p}{\partial \delta_p} = -Q_p - B_{pp}|V_p|^2 \tag{4.9}$$

Assuming $Q_p << |V^2|B_{pp}$ in (4.9) yields

$$\frac{\partial P_p}{\partial \delta_p} = -B_{pp}|V_p|^2 \tag{4.10}$$

From the expression for diagonal elements of L submatrix, (2.24), we have

$$\frac{\partial P_p}{\partial \delta_p} = \frac{\partial Q_p}{\frac{\partial |V_p|}{|V_p|}} = -B_{pp}|V_p|^2 \tag{4.11}$$

Using (4.8) and (4.11) in (4.3) and (4.4), and expanding, we get

$$\begin{bmatrix} -|V_1V_1|B_{11} & -|V_1V_2|B_{12} & \cdots & -|V_1V_n|B_{1n} \\ -|V_2V_1|B_{21} & -|V_2V_2|B_{22} & \cdots & -|V_2V_n|B_{2n} \\ \vdots & \vdots & \vdots & \vdots \\ -|V_nV_1|B_{n1} & -|V_nV_2|B_{n2} & \cdots & -|V_nV_n|B_{nn} \end{bmatrix} \begin{bmatrix} \triangle\delta_1 \\ \triangle\delta_2 \\ \vdots \\ \triangle\delta_n \end{bmatrix} = \begin{bmatrix} \triangle P_1 \\ \triangle P_2 \\ \vdots \\ \triangle P_n \end{bmatrix} \tag{4.12}$$

and

$$\begin{bmatrix} -|V_1V_1|B_{11} & -|V_1V_2|B_{12} & \cdots & -V_1V_n|B_{1n} \\ -|V_2V_1|B_{21} & -|V_2V_2|B_{22} & \cdots & -|V_2V_n|B_{2n} \\ \vdots & \vdots & \vdots & \vdots \\ -|V_nV_1|B_{n1} & -|V_nV_2|B_{n2} & \cdots & -|V_nV_n|B_{nn} \end{bmatrix} \begin{bmatrix} \frac{\triangle|V_1|}{|V_1|} \\ \frac{\triangle|V_2|}{|V_2|} \\ \vdots \\ \frac{\triangle|V_n|}{|V_n|} \end{bmatrix} = \begin{bmatrix} \triangle Q_1 \\ \triangle Q_2 \\ \vdots \\ \triangle Q_n \end{bmatrix} \tag{4.13}$$

(4.14)

Now, the first row of the coefficient matrix in (4.13) is multiplied by the correction vector and then it is divided by $|V_1|$ to obtain,

$$-B_{11}\triangle|V_1| \quad -B_{12}\triangle|V_2| \quad \cdots \quad -B_{1n}\triangle|V_n| = \frac{\triangle Q_1}{|V_1|} \tag{4.15}$$

Each row of (4.13) can be similarly treated by representing the reactive power mismatch at bus p by the quantity $\frac{\triangle Q_P}{|V_P|}$, where, $p = 1, 2, \ldots, n$. With these, (4.13) is modified as

$$\begin{bmatrix} -B_{11} & -B_{12} & \cdots & -B_{1n} \\ -B_{21} & -B_{22} & \cdots & -B_{2n} \\ \vdots & \vdots & \vdots & \vdots \\ -B_{n1} & -B_{n2} & \cdots & -B_{nn} \end{bmatrix} \begin{bmatrix} \triangle|V_1| \\ \triangle|V_2| \\ \vdots \\ \triangle|V_n| \end{bmatrix} = \begin{bmatrix} \frac{\triangle Q_1}{|V_1|} \\ \frac{\triangle Q_2}{|V_2|} \\ \vdots \\ \frac{\triangle Q_n}{|V_n|} \end{bmatrix} \tag{4.16}$$

Using the first row of the coefficient matrix in (4.12) we have,

$$-|V_1|B_{11}\triangle\delta_1 \quad -|V_2|B_{12}\triangle\delta_2 \quad \cdots \quad -|V_n|B_{1n}\triangle\delta_n = \frac{\triangle P_1}{|V_1|} \tag{4.17}$$

Applying the above steps to the remaining rows of the coefficient matrix, we get,

$$\begin{bmatrix} -|V_1|B_{11} & -|V_2|B_{12} & \cdots & -|V_n|B_{1n} \\ -|V_1|B_{21} & -|V_2|B_{22} & \cdots & -|V_n|B_{2n} \\ \vdots & \vdots & \vdots & \vdots \\ -|V_1|B_{n1} & -|V_2|B_{n2} & \cdots & -|V_n|B_{nn} \end{bmatrix} \begin{bmatrix} \triangle\delta_1 \\ \triangle\delta_2 \\ \vdots \\ \triangle\delta_n \end{bmatrix} = \begin{bmatrix} \frac{\triangle P_1}{|V_1|} \\ \frac{\triangle P_2}{|V_2|} \\ \vdots \\ \frac{\triangle P_n}{|V_n|} \end{bmatrix} \tag{4.18}$$

The coefficient matrix in (4.18) is made the same as that in (4.16) by setting $|V_2|$,$|V_2|$, $\cdots$ $|V_n|$ equal to 1.0 pu in the left hand side expression of (4.18). With these modification, we get

$$\begin{bmatrix} -B_{11} & -B_{12} & \cdots & -B_{1n} \\ -B_{21} & -B_{22} & \cdots & -B_{2n} \\ \vdots & \vdots & \vdots & \vdots \\ -B_{n1} & -B_{n2} & \cdots & -B_{nn} \end{bmatrix} \begin{bmatrix} \triangle\delta_1 \\ \triangle\delta_2 \\ \vdots \\ \triangle\delta_n \end{bmatrix} = \begin{bmatrix} \frac{\triangle P_1}{|V_1|} \\ \frac{\triangle P_2}{|V_2|} \\ \vdots \\ \frac{\triangle P_n}{|V_n|} \end{bmatrix} \tag{4.19}$$

In FDLF method, the $P-\delta$ equation, (4.19) and $Q-|V|$ equation, (4.16) are written in a compact form as:

$$\left[\frac{\triangle \underline{P}}{|\underline{V}|}\right] = [B'][\triangle\underline{\delta}] \tag{4.20}$$

$$\left[\frac{\triangle \underline{Q}}{|\underline{V}|}\right] = [B'']\left[\triangle|\underline{V}|\right] \tag{4.21}$$

Where B' and B'' are susceptances matrices and are obtained as negative imaginary part of bus admittance matrix. The correction vectors $\triangle\underline{\delta}$ and $\triangle|\underline{V}|$ are obtained by solving (4.20) and (4.21) respectively. These corrections are used to update the angle and voltage magnitude at bus p in k^{th} iteration as follows:

$$\delta_p^K = \delta_p^{(K-1)} + \triangle\delta_p^{(K-1)} \tag{4.22}$$

$$|V_p^K| = |V_p^{(K-1)}| + |\triangle V_p^{(K-1)}| \tag{4.23}$$

4.2.1 Formation of B' and B'' Matrices:

Some of the typical formulations of $B' - B''$ matrices, in order, are B-B, B-X, X-B and X-X type [16]. The letter B represents the inclusion of both the branch resistances and reactances in the formation of coefficient matrix and the letter X indicates construction of coefficient matrix by neglecting the branch resistances. In this paper, the standard X-B-version is considered for the formulation of B' and B'' matrices because of its excellent convergence properties under normal operating conditions [17].

Formation of B' Matrix:

Form Y_d with the following assumptions:

1. Omit the representation of those network elements that predominantly affect MVAr flows, i.e., shunt susceptances (inductive or capacitive) if any, line charging, and off-nominal in-phase transformer taps.
2. Neglect series resistances.

Then

$$B' = -\text{Im}[Y_d]$$

Note that B' does not contain the row and column corresponding to slack bus and its size is $(n-1) \times (n-1)$.

Formation of B'' Matrix:

Construct Y_{BUS} after neglecting the effect of phase shifters, if any and then

$$B'' = -\text{Im}[Y_{BUS}]$$

Note that B'' does not contain rows and columns corresponding to slack and PV-buses and its size is $(n-m-1) \times (n-m-1)$.

4.3 FDLF Implementation Algorithm:

There are two types of schemes available for the implementation of FDLF method, these are as follows:

1. Selective iteration scheme [7]: In this approach, $\triangle \underline{P}$ and $\triangle \underline{Q}$ mismatches are verified individually for convergence. This leaves the possibility to skip one or more $P - \delta$ and/or $Q - |V|$ iterations as soon as the related power mismatches are converged.

2. Successive iteration scheme [16, 18]: In this approach, both $\triangle\underline{P}$ and $\triangle\underline{Q}$ are verified at a time for convergence, i.e., if $\triangle\underline{P}$ convergence has reached early compared to $\triangle\underline{Q}$ convergence, even then $P-\delta$ cycle is repeated until the $\triangle\underline{Q}$ convergence has reached.

In the following sections, the FDLF schemes have been demonstrated with and without accounting Q-limits at PV-buses, only for *selective iteration scheme*.

4.3.1 PV-buses Without Q-limits Specifications:

The implementation steps are depicted in flow chart shown in Figure 4.1. The flow chart also shows the provision made for the inclusion of Q-limits at PV-buses and voltage- and frequency-dependent load models in the normal FDLF method [19]. In this case set 'Q-bit' = 0, 'VM-bit' = 0 and 'FM-bit'= 0. This setting by-passes the load model routine [(C)-(D)], and Q-limit imposing routine [(X)-(Y)].

4.3.1.1 Load Flow Study Example:

The sample 4 bus system shown in Figure 2.2 is used to demonstrate the FDLF method without accounting Q-limits at PV-buses.

1. Construct the bus admittance matrix Y_{BUS} as usual.

$$\begin{bmatrix} 8.9852-j44.8360 & -3.8156+j19.0781 & -5.1696+j25.8478 & 0 \\ -3.8156+j19.0781 & 8.9852-j44.8360 & 0 & -5.1696+j25.8478 \\ -5.1696+j25.8478 & 0 & 8.1933-j40.8638 & -3.0237+j15.1185 \\ 0 & -5.1696+j25.8478 & -3.0237+j15.1185 & 8.1933-j40.8638 \end{bmatrix}$$

   Using this bus admittance matrix, B'' matrix is obtained by removing rows and columns corresponding to PV-bus and slack bus as:

$$B'' = \begin{bmatrix} 44.8360 & 0 \\ 0 & 40.8638 \end{bmatrix}$$

2. Construct the bus admittance matrix Y_d, following the assumptions explained in section (4.2.1).

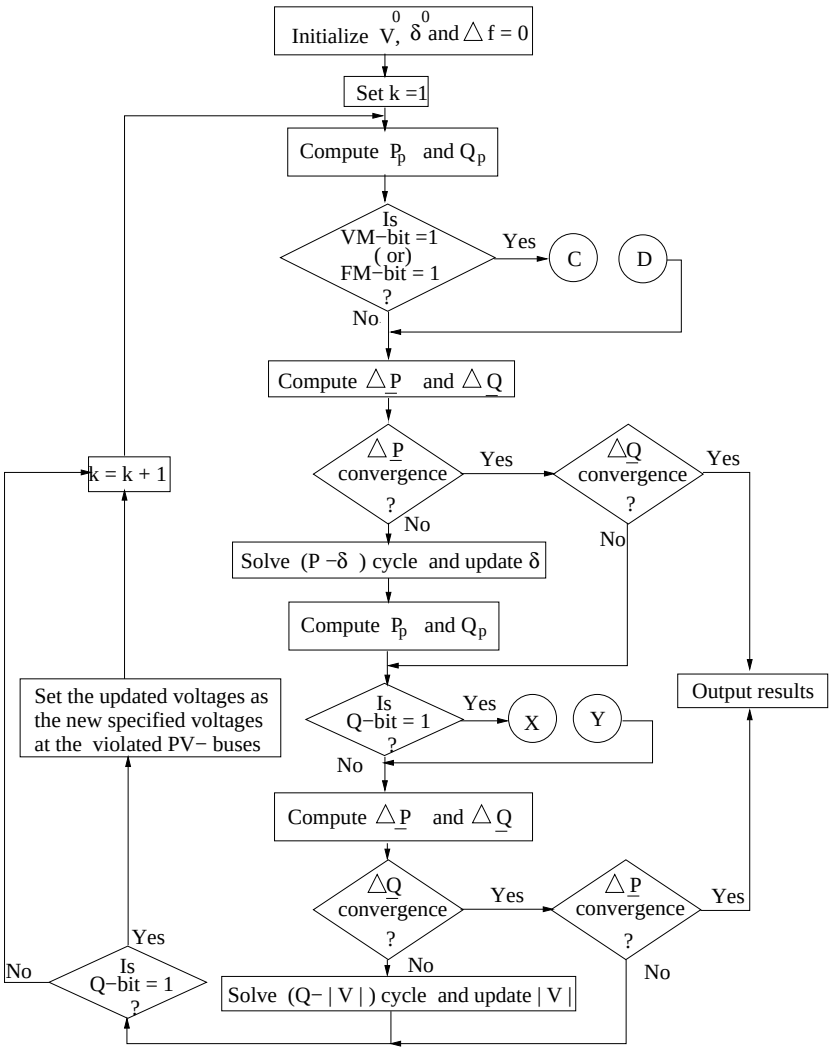

Figure 4.1: Flow chart for the modified FDLF selective iteration scheme.

$$Y_d = \begin{bmatrix} 0 - j46.723 & 0 + j19.8413 & 0 + j26.8817 & 0 \\ 0 + j19.8413 & 0 - j46.7230 & 0 & 0 + j26.8817 \\ 0 + j26.8817 & 0 & 0 - j42.6050 & 0 + j15.7233 \\ 0 & 0 + j26.8817 & 0 + j15.7233 & 0 - j42.6050 \end{bmatrix}$$

Using this bus admittance matrix, B' matrix is obtained by removing the row and column corresponding to the slack bus as:

$$B' = \begin{bmatrix} 46.7230 & 0 & -26.8817 \\ 0 & 42.6050 & -15.7233 \\ -26.8817 & -15.7233 & 42.6050 \end{bmatrix}$$

Iteration 1:

1. The specified bus powers and the bus powers calculated (using the initial bus voltages) are :

Bus No. p	P_p^{sp}	P_p	$\frac{\triangle P_p}{\|V_p\|}$
2	-1.7	-0.1034	-1.5966
3	-2.0	-0.0605	-1.9395
4	2.38	0.1671	2.2129

2. Using the computed real power mismatches and the elements of B' matrix, we solve (4.20), to get the angle correction vector as:

Bus No. p	2	3	4
$\triangle\delta_p$ (deg)	-1.1312	-2.0780	1.4369

3. Using the updated angles, the computed reactive power mismatches are:

Bus No. p	Q_p^{sp}	Q_p	$\frac{\triangle Q_p}{\|V_p\|}$
2	1.0535	-0.2652	-0.7883
3	1.2394	0.0177	-1.2571

4. Using the computed reactive power mismatches and the elements of B'' matrix, we solve (4.21), to get the voltage magnitude correction vector and the voltage magnitude vector as:

Bus No. p	2	3
$\|\triangle V_p\|$ (pu)	-0.0176	-0.0308
$\|V_p\|$(pu)	0.9824	0.9692

At the end of 3^{rd} iteration (both $P-\delta$ and $Q-|V|$ cycle):

The specified bus powers and the bus powers calculated (using the updated bus voltages at the end of 3^{rd} iteration) are:

Bus No.p	P_p^{sp}	P_p	ΔP_p	Q_p^{sp}	Q_p	ΔQ_p
2	-1.70	-1.7000	0	-1.0535	-1.0535	0.000
3	-2.0	-2.0001	0.0001	-1.2394	-1.2394	0.000
4	2.38	2.3801	0.0001	-	-	-

From the above table, it is observed that the calculated bus power mismatches fall below ϵ. The converged results are shown in Table 4.1.

Bus No. p No	$\|V_p\|$ (pu)	δ_p (deg)	P_{Gp} (pu)	Q_{Gp} (pu)	P_{Lp} (pu)	Q_{Lp} (pu)
1	1.000000	0.000000	1.868101	1.145057	0.500000	0.309900
2	0.982421	-0.976037	0.000000	0.000000	1.700000	1.053500
3	0.969003	-1.872244	0.000000	0.000000	2.000000	1.239400
4	1.020000	1.523196	3.180000	1.814320	0.800000	0.495800

Table 4.1: Converged load flow results without Q-limits (Selective iteration scheme).

4.3.2 PV-buses With Q-limits Specifications:

In FDLF method, the Q-limits at PV-buses are handled by a way of bus-type switching (see section 1.2.2) as is implemented in the N-R method. Here, instead of iteration count, the reactive power mismatch at PQ-buses ($max|\Delta \underline{Q}| \leq 0.1$) is used as the starting criteria since it provides a direct way to control the degree of convergence [9]. It is observed that the enforcement of Q-limit specifications at PV-buses by a way of bus-type switching, causes an oscillatory convergence. To overcome these convergence difficulties, a procedure which is a combination of the bus-type switching and adjusting the specified voltage at PV-buses, is suggested to the standard FDLF. The adjustment procedure is as follows:

- Following Q-limit violations at PV-buses in a certain iterative step, the buses are switched to PQ-type and the voltage corrections at those buses are calculated by solving $Q - |V|$ cycle.
- The obtained voltage corrections are used to adjust the bus voltages at the violated PV-buses.
- The adjusted bus voltages are set as the new specified voltages at the PV-buses for the next iteration. This implies that the back-offs at PV-buses are neglected. This is justified based on the observation made in [9] that the number of back-offs is normally small when Q-limits are enforced after the solution has moderately converged.

With the above cited steps, Figure 2.3 is modified as shown in Figure 4.2 and the modified scheme is enabled in Figure 4.1 by setting 'Q-bit' = 1. The variable, `Qstart_cri` is set to 0.1 in the programme `fdlf_jacob_form.m`

4.3.2.1 Load Flow Study Example:

The sample 4 bus system shown in Figure 2.2 is used to demonstrate the FDLF method accounting Q-limits at PV-buses using selective iteration scheme. The 'Q-bit' is set to 1,

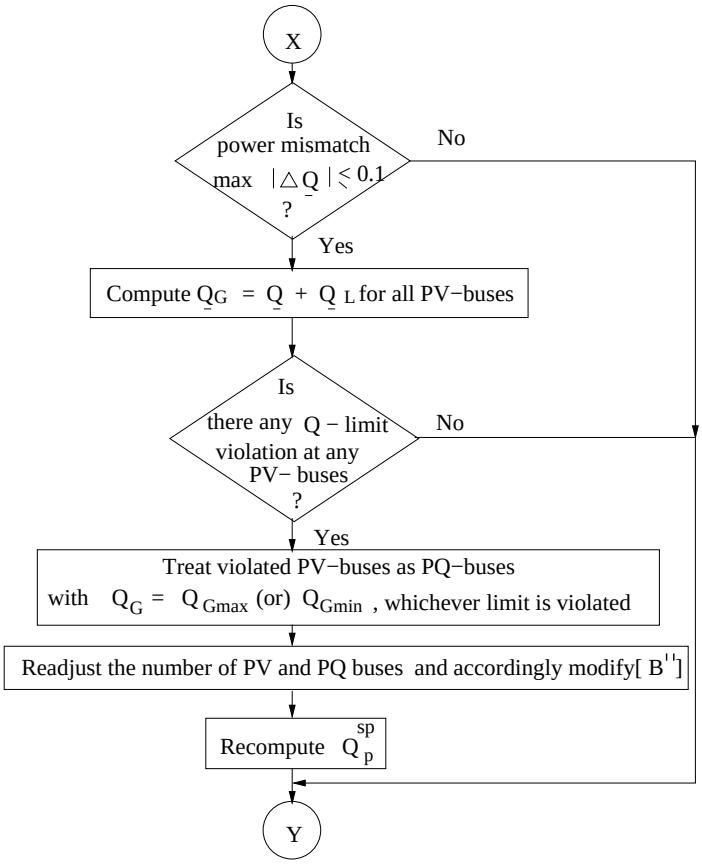

Figure 4.2: Flow chart for modified bus-type switching logic for FDLF.

and 'VM-bit' and 'FM-bit' are set to 0.

Iteration 1:

The bus voltage magnitudes and angles at the end of 1^{st} P- and Q-iteration are as follows:

Bus No. p	1	2	3	4
$\|V_p\|$	1.00	0.9824	0.9692	1.02
δ_p	0	-1.1312	-2.0780	1.4369

It is observed that the enforcement of Q-limits takes place at the beginning of 2^{nd} Q-iteration. Therefore, the steps involved in the above calculation are identical to that of 1^{st} iteration in a case where Q-limits are not accounted at PV-buses (see section 4.3.1.1).

Iteration 2

1. The specified bus powers and the bus powers calculated (using the updated bus voltages at the end of 1^{st} P- and Q-iteration) are:

Bus No. p	P_p^{sp}	P_p	$\frac{\triangle P_p}{\|V_p\|}$
2	-1.7	-1.7814	0.0829
3	-2.0	-2.1188	0.1225
4	2.38	2.4425	-0.0612

2. Using the computed bus power mismatches and the elements of B' we have (as per (4.20),

$$\begin{bmatrix} 0.0829 \\ 0.1225 \\ -0.0612 \end{bmatrix} = \begin{bmatrix} 46.7230 & 0 & -26.8817 \\ 0 & 42.6050 & -15.7233 \\ -26.8817 & -15.7233 & 42.6050 \end{bmatrix} \begin{bmatrix} \triangle\delta_2 \\ \triangle\delta_3 \\ \triangle\delta_4 \end{bmatrix} \tag{4.24}$$

3. Solving the above equation, we get the angle corrections and updated bus angles as:

Bus No p	2	3	4
$\triangle\delta_p$ (deg)	0.1505	0.1961	0.0850
δ_p(deg)	-0.9807	-1.8819	1.5219

4. Recomputed reactive power mismatches $\triangle\underline{Q}$ (using updated angles) are

Bus No. p	Q_p^{sp}	Q_p	$\frac{\triangle Q_p}{\|V_p\|}$
2	-1.0536	-1.0530	-0.0006
3	-1.2397	-1.2289	-0.0108
4	-	1.3144	-

From the above tabulated values of $\triangle Q_p$, it is observed that the $max|\triangle\underline{Q}| < 0.1$. Therefore, enforcement of Q-limits takes place now as per the flow chart given in Figure 4.2. At bus 4, the real power load is $P_{L4} = 0.8$ pu. and reactive power load is $Q_{L4} = 0.4958$ pu. While checking the Q-limits at PV bus, the required reactive power generation is calculated as: $Q_{G4} = Q_4 + Q_{L4} = 1.3144 + 0.4958 = 1.8102$ pu. Note that $Q_{G4} > Q_{Gmax}$ (= 0.4 pu.). Therefore, this bus is treated as a PQ-bus with $Q_{G4} = 0.4$ pu. with the initial bus voltage magnitude as $|V_4| = 1.02$ pu. Due to this, the number of PQ-buses are 3. Further, $Q_4^{sp} = Q_{G4} - Q_{L4} = 0.4$ - 0.4958 = -0.0958. $\Delta Q_4 = Q_4^{sp} - Q_4 =$ -0.0958 -1.3144 = 1.4102. And $\frac{\Delta Q_4}{|V_4|} = 1.3826$. Accordingly, the B'' matrix is modified as:

$$B'' = \begin{bmatrix} 44.8360 & 0 & -25.8478 \\ 0 & 40.8638 & -15.1185 \\ -25.8478 & -15.1185 & 40.8638 \end{bmatrix}$$

5. Using the computed bus power mismatches and the elements of B'' we have (as per (4.21),

$$\begin{bmatrix} -0.0006 \\ -0.0108 \\ -1.3826 \end{bmatrix} = \begin{bmatrix} 44.8360 & 0 & -25.8478 \\ 0 & 40.8638 & -15.1185 \\ -25.8478 & -15.1185 & 40.8638 \end{bmatrix} \begin{bmatrix} \triangle V_2 \\ \triangle V_3 \\ \triangle V_4 \end{bmatrix} \tag{4.25}$$

6. Solving the above equation, we get

Bus No. p	2	3	4
$\lvert\triangle V_p\rvert$	-0.0393	-0.0255	-0.0681
$\lvert V_p\rvert$	0.9432	0.9438	0.9519

7. Now, set $|V_4^{sp}| = 0.9519$ pu. for the next iterations.

At the end of 5^{th} iteration: The specified bus powers and the bus powers calculated (using the updated bus voltages at the end of 5^{th} iteration) are:

Bus No.p	P_p^{sp}	P_p	ΔP_p	Q_p^{sp}	Q_p	ΔQ_p
2	-1.7	-1.6998	0.0002	-1.0535	-1.0528	-0.0007
3	-2.0	-1.9998	0.0002	-1.2394	-1.2388	-0.0006
4	2.38	2.3796	0.0004	-	-0.0963	-

From above table, it is observed that the bus power mismatches fall below ϵ. Further, it is found that the Q-limit constraints at bus 4 are almost satisfied at this point ($Q_{G4} = -0.0963 + 0.4958 = 0.3995$). In this example, $\triangle\underline{Q}$ mismatch reaches convergence at the end of 4^{th} iteration. And $\triangle\underline{P}$ convergence has reached at the end of 5^{th} iteration. Converged load flow results are as follows:

Bus No.p	$\lvert V_p\rvert$ (pu)	δ_p (deg)	P_{Gp} (pu)	Q_{Gp} (pu)	P_{Lp} (pu)	Q_{Lp} (pu)
1	1.000000	0.000000	1.884557	2.666903	0.500000	0.309900
2	0.941405	-0.533504	0.000000	0.000000	1.700000	1.053500
3	0.942331	-1.631538	0.000000	0.000000	2.000000	1.239400
4	0.951528	2.635645	3.180000	0.399517	0.800000	0.495800

Table 4.2: Converged load flow results with Q-limits (Selective iteration scheme)

4.3.3 Convergence Results for the IEEE Systems:

The results obtained using the IEEE test systems [13, 14] are presented in Tables 4.3 and 4.4. Base used is 100 MVA. The approximate execution time is obtained in a P4 computer (3 GHz, 512 MB DDR 400 MHz memory, 910 GL chipset) and it also includes the time for report generation.

IEEE system	P-iter	Q-iter.	Execution time (s)
14-bus	3	3	0.032
30-bus	3	3	0.032
57-bus	4	3	0.047
118-bus	4	3	0.078
145-bus	9	7	0.156
162-bus	4	3	0.109
300-bus	6	5	0.157

Table 4.3: IEEE test system results without accounting Q-limits at PV-buses (FDLF).

IEEE system	P-iter	Q-iter.	Execution time (s)
14-bus	3	3	0.032
30-bus	3	3	0.032
57-bus	4	3	0.047
118-bus	4	3	0.063
300-bus	6	5	0.156

Table 4.4: IEEE test system results accounting Q-limits at PV-buses (FDLF).

4.4 Handling of Static Load Models in Load Flows

To account load modelling in load flow programmes, polynomial expression-based static load model has been employed, where voltage- and frequency-dependency of loads have been considered [20]-[22]. The procedure involved has been discussed in the following lines.

1. Voltage-dependent load models: Here the term P_{Lp} (i.e., real power load at bus p) in the specified real power expression given by $P_p^{sp} = P_{Gp} - P_{Lp}$, is replaced by the polynomial expression for real power as:

$$P_{Lp} = P_{Lop}\left\{a_{1p} + a_{2p}\left(\frac{|V_p|}{|V_{op}|}\right) + a_{3p}\left(\frac{|V_p|}{|V_{op}|}\right)^2\right\} \tag{4.26}$$

Similarly, the reactive power load at bus p, Q_{Lp} is given by

$$Q_{Lp} = Q_{Lop}\left\{b_{1p} + b_{2p}\left(\frac{|V_p|}{|V_{op}|}\right) + b_{3p}\left(\frac{|V_p|}{|V_{op}|}\right)^2\right\} \tag{4.27}$$

where, P_{Lop} and Q_{Lop} are nominal values of active and reactive components of load powers at nominal voltage $|V_{op}|$. a_1 to a_3 and b_1 to b_3, are coefficients of voltage-dependent real and reactive power loads at bus p with

$$a_{1p} + a_{2p} + a_{3p} = 1$$
$$b_{1p} + b_{2p} + b_{3p} = 1$$

2. Frequency-dependent load models: Here the term P_{Lp} (i.e., real power load at bus p) is replaced by P_{Lfp} and is given as:

$$P_{Lfp} = P_{Lp}\left[1 + K_{pf}\triangle\underline{f}\right] \tag{4.28}$$

Similarly, the term Q_{Lp} is replaced by Q_{Lfp} and is given as:

$$Q_{Lfp} = Q_{Lp}\left[1 + K_{qf}\triangle\underline{f}\right] \tag{4.29}$$

where, K_{pf} and K_{qf} are coefficients of frequency-dependent real and reactive power loads at bus p.

Incorporation of frequency-dependent load models in load flow studies can be implemented by knowing the specified real power generation at slack bus, P_{Gs}^{sp}. The implementation procedure is as follows:

(a) Compute the slack bus real power generation $P_{Gs} = P_s + P_{Ls}$, where, P_s represents the computed real power at slack bus, P_{Ls} represents the real power load at slack bus if any.

(b) Initialize the per unit frequency deviation $\triangle\underline{f} = 0$

(c) Compute the frequency-deviation correction factor ($\triangle F_c$) using,

$$\triangle F_c = (P_{Gs}^{sp} - P_{Gs}) \times C_f \tag{4.30}$$

where C_f is referred to as a frequency convergence factor and is selected appropriately for a given system.

(d) Update the frequency-deviation $\triangle\underline{f}$, in k^{th} iterative step as

$$\triangle\underline{f}^k = \triangle\underline{f}^{(k-1)} + \triangle F_c^k$$

(e) Use the updated $\triangle \underline{f}$, in (4.28 and 4.29).

(f) Compute the system frequency $f = f_o(1 + \Delta \underline{f})$, where f_o is the nominal frequency.

(g) While checking for convergence, the real power generation mismatch at slack bus is also considered.

NOTE:

- The value of C_f is chosen so as to provide the minimum possible number of iterations. This value is system dependent and is to be decided by trail and error method. To get an approximate *initial* value of C_f, the following rule-of-thumb may be used:

$$C_f = \frac{1}{10}\left(\frac{P_{Gs}^{sp}}{\sum\limits_{all\ \ loads} P_{Lop}}\right)$$

- The governor characteristics are not modelled.

Thus, the specified bus power itself becomes a function of voltage magnitude and frequency deviation and it varies from iteration to iteration. This in turn is used to calculate the bus power mismatches in the solution process. The implementation flowchart for handling the load models in load flows is given in Figure 4.3. 'VM-bit' and 'FM-bit' are set to 1 or 0, if voltage- and/or frequency-dependent load models are to be considered. Refer Figure 4.1 for the complete flowchart.

Test results are obtained are tabulated in Table 4.5 considering Q-limits at PV-buses with voltage- and frequency-dependent load models for all loads. This is done by setting 'Q-bit' = 1, 'VM-bit' = 1 and 'FM-bit' = 1. The load model parameters used are $a_1 = 0.4$, $a_2 = 0.3$ and $a_3 = 0.3$ for real power loads and $b_1 = 0.4$, $b_2 = 0.3$, and $b_3 = 0.3$ for reactive power loads. In addition, K_{pf} and K_{qf} are set to 2 and -1.5, respectively. The nominal frequency is 50 Hz.

IEEE system	P_{Gs}^{sp} pu	C_f	f (Hz)	P-itr	Q-itr	Time s
14-bus	2.3715	0.1	50.0194	7	6	0.063
30-bus	2.6389	0.15	49.9700	8	7	0.078
118-bus	4.9048	0.01	49.9994	5	4	0.093
300-bus	4.5337	0.001	50.0003	14	11	0.281

Table 4.5: Study results with voltage- and frequency-dependent load models.

The specified nominal real power generation at the slack bus (P_{Gs}^{sp}) is obtained for the base case loads accounting voltage-dependent loads and Q-limits at PV-buses.

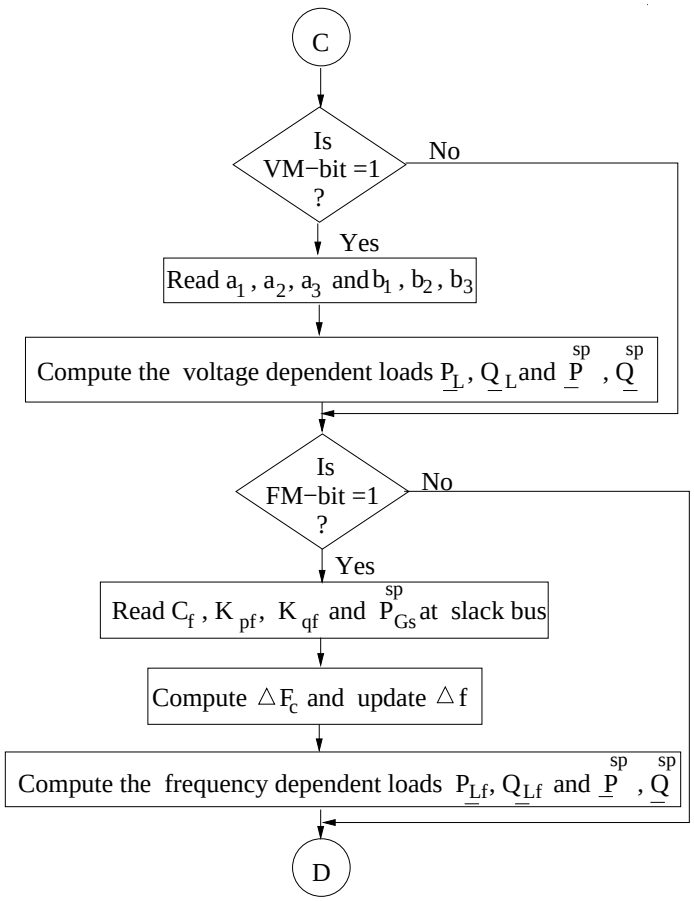

Figure 4.3: Implementation of load modelling module in load flow.

NOTE:

The execution time indicated are not exact and is used for comparison purpose only. These values are obtained using an in-built MATLAB function, `etime` and `clock`.

4.5 Representation HVDC Systems For Power Flow Solution:

Power flow analysis requires joint solution of the DC and AC system of equations. The sequential approach where solution is alternated between single AC and DC iterations is employed [23]-[27]. In this method, the AC and DC link equations are solved separately and thus the integration into the standard load flow program is carried out without significant modifications of the AC load flow algorithm. The flow of various variables between DC and AC solutions are illustrated in Figure 4.4.

Here, E_{acr} and E_{aci} are considered to be the input quantities for the solution of DC system equations. They are known from the previous AC iteration. Using these bus

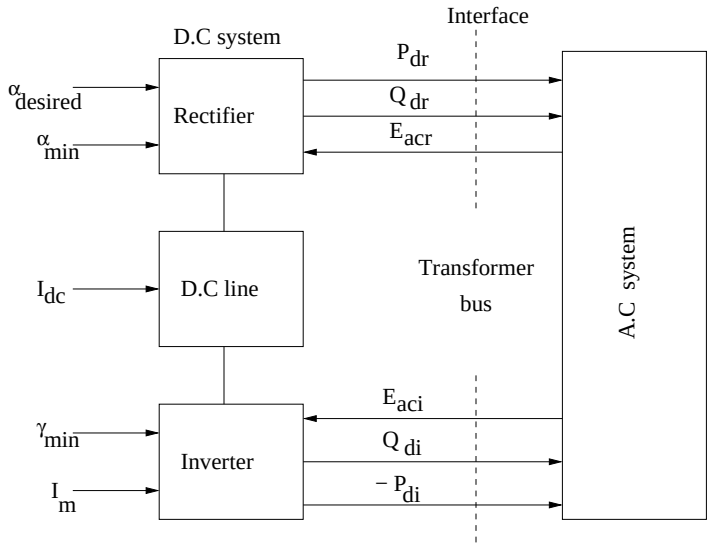

Figure 4.4: Block diagram to illustrate the interfacing of DC system with AC system in load flow.

voltages the converter bus powers, P_{dr}, Q_{dr}, P_{di} and Q_{di} are computed and are treated as fictitious loads at the converter buses in the next iteration for solving the AC system equations. This process is repeated until convergence is reached in AC iterations.

The basic converter equations, for both rectifier and inverter operations, describing the relationship between the AC and DC variables are given below [12]:

$$\begin{aligned} V_{do} &= \frac{3\sqrt{2}}{\pi} B\ T\ E_{ac} \\ V_{dr} &= V_{dor}\cos\alpha - \frac{3}{\pi}X_{cr}I_d B_r \\ V_{di} &= V_{doi}\cos\gamma - \frac{3}{\pi}X_{ci}I_d B_i \\ \Phi &= \cos^{-1}(V_d/V_{do}) \\ P_d &= V_d I_d \\ Q_d &= P_d \tan\Phi \end{aligned} \tag{4.31}$$

where, V_{do} is the ideal no-load direct voltage, α is the rectifier ignition delay angle, γ is the inverter extinction advance angle, ϕ is the phase angle between the AC voltage E_{ac} and the fundamental AC current (i.e. power factor angle), $R_c = \frac{3}{\pi}X_c$ is the commutating resistance per bridge/phase, X_c is the leakage reactance of the converter transformer/phase, B is the number of series connected bridges in each converter, T is the converter transformer tap-ratio, T_n represents nominal tap setting. N denotes the number of tap positions, R_{dc} represents resistance of the DC line and I_m is the specified current margin.

4.5.1 DC Link Specification Schemes

The basic variables per converter are $V_d, \alpha(\gamma)$, T, ϕ, P_d and Q_d, and the variable I_d is common to both converters. Thus in all, there are 13 variables available for any two-terminal DC link. Two major specification schemes that are generally employed in DC systems to solve for unknown variables, are as follows:

1. DC link-current specification : In this case, the link-current, I_{dc}^{sp} is specified.
2. DC link-power specification : In this case, either rectifier-end DC power P_{dr} or inverter-end DC power P_{di} is specified.

In each of the above specifications, other variables such as α, V_{dr}, T_r at rectifier, and γ, V_{di}, T_i at inverter may be specified. Thus, it may lead to many combinations of the specified variable set. The solution of DC link equations will be different for each of the specification set [28]. In this paper, the following specification sets are used:

1. I_{dc}^{sp} and V_{di}^{sp} are specified.
2. P_{dr}^{sp} and V_{di}^{sp} are specified.

The dependent and independent variables in the solution of DC equations depend on the mode of operation of converters. For a given power direction, generally, 3 modes of operations are defined: *Mode-1*: rectifier is on constant current (CC) control and inverter is on constant extinction angle (CEA) control, *Mode-2*: rectifier is on constant ignition angle (CIA) control and inverter is on constant current (CC) control, and *Mode-3*: rectifier is on constant ignition angle (CIA) control and inverter is on constant extinction angle (CEA) control. It is found that in power flow studies it is usually sufficient to consider *Mode-1* and *Mode-2* [12]. For any given system conditions, the rectifier and inverter modes of operation may not be known prior to the solutions of system equations. The following procedure has been adopted to identify the mode of operation of a converter (see Figure 4.5):

1. Knowing AC side bus voltages, compute α using the following expression.

$$\alpha = \cos^{-1}\left(\frac{V_{dr} + R_{cr}B_r I_d}{V_{odr}}\right) \tag{4.32}$$

2. If $\alpha > \alpha_{min}$, *Mode-1* condition is satisfied.
3. If $\alpha \leq \alpha_{min}$, *Mode-2* condition is satisfied.

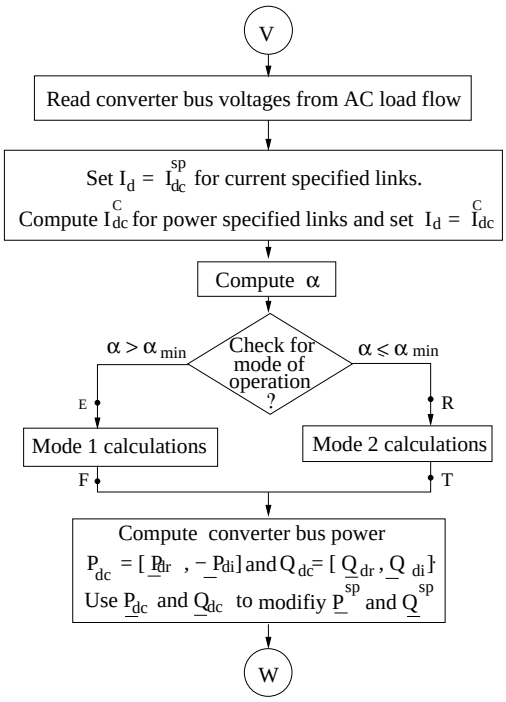

Figure 4.5: Flowchart of DC module.

4.5.2 Solution of DC Link Equations

DC link-current specification:

Having specified I_{dc}^{sp} and V_{di}^{sp}, it is possible to solve for the remaining unknown variables with the knowledge of the AC voltages. The steps involved in *Mode-1* and *Mode-2* are as follows:

1. Initially set $V_{dr} = V_{drn}$, where V_{drn} is the nominal rectifier-end DC voltage.
2. Compute α using (4.32) with $I_d = I_{dc}^{sp}$ and identify the mode of operation.
3. Perform *Mode-1* and/or *Mode-2* calculations using (4.39) or (4.40) for each link.

Rectifier-end DC power specification:

Having specified P_{dr}^{sp} and V_{di}^{sp}, it is possible to solve for the remaining unknown variables with the knowledge of the AC voltages. The steps involved are as follows:

1. Compute the DC link current order I_{dc}^{C} knowing P_{dr}^{sp} and V_{di}^{sp}. The equations used in the computation of DC current I_{dc}^{C} are :

$$P_{di} = V_{di}^{sp}\ I_{dc}^{C} \tag{4.33}$$

$$P_{dr}^{sp} = P_{di} + \left(I_{dc}^{C}\right)^2\ R_{dc} \tag{4.34}$$

Solving (4.33) and (4.34), we get a feasible expression for I_{dc}^{C} as,

$$I_{dc}^{C} = \frac{1}{2R_{dc}} \left[-V_{di}^{sp} + \sqrt{(V_{di}^{sp})^2 + 4\ P_{dr}^{sp}\ R_{dc}} \right] \tag{4.35}$$

2. Initially set $V_{dr} = V_{drn}$, and compute α using (4.32) with $I_d = I_{dc}^{C}$ and identify the mode of operation.

3. Perform *Mode-1* or *Mode-2* calculations using (4.39) or (4.40) for each link.

The expression that is used to calculate DC link-current order in *Mode-2* is obtained as follows:

We know that in *Mode-2*,

$$P_{dr}^{sp} = V_{dr}\ I_d \tag{4.36}$$

$$V_{dr} = V_{dor} \cos \alpha_{min} - R_{cr} B_r I_d \tag{4.37}$$

Using (4.36) and (4.37), and solving for a feasible I_d, we get

$$I_d = \frac{1}{2R_{dc}} \left[V_{dor} \cos \alpha_{min} - \sqrt{(V_{dor} \cos \alpha_{min})^2 - 4 P_{dr} R_{cr}} \ \right] \tag{4.38}$$

1. *Mode-1* calculation:

$$\begin{aligned} I_d &= I_{dc}^{sp} \text{ for current specification.} \\ I_d &= I_{dc}^{C} \text{ for power specification, see (4.35).} \end{aligned}$$

$$\begin{aligned} T_i &= \frac{V_{di}^{sp} + R_{ci} B_i I_d}{\frac{3\sqrt{2}}{\pi} B_i E_{aci} \cos \gamma_{min}} \\ V_{doi} &= \frac{3\sqrt{2}}{\pi} B_i T_i E_{aci} \\ \phi_i &= \cos^{-1}(V_{di}^{sp}/V_{doi}) \\ P_{di} &= V_{di}^{sp} I_d \\ Q_{di} &= P_{di} \tan \phi_i \\ V_{dr} &= V_{di}^{sp} + R_{dc} I_d \\ V_{dor} &= \frac{3\sqrt{2}}{\pi} B_r T_r E_{acr} \\ \alpha &= \cos^{-1} \left(\frac{V_{dr} + R_{cr} B_r I_d}{V_{odr}} \right) \\ \phi_r &= \cos^{-1}(V_{dr}/V_{dor}) \\ P_{dr} &= V_{dr} I_d \\ Q_{dr} &= P_{dr} \tan \phi_r \end{aligned} \tag{4.39}$$

2. *Mode-2* calculations:

$$I_d = I_{dc}^{sp} - I_m \quad \text{for current specification.}$$
$$I_d \quad \text{is obtained using (4.38), for power specification.}$$

$$\begin{aligned}
V_{dor} &= \frac{3\sqrt{2}}{\pi} B_r T_r E_{acr} \\
V_{dr} &= V_{dor}\cos\alpha_{min} - R_{cr} B_r I_d \\
\phi_r &= \cos^{-1}(V_{dr}/V_{dor}) \\
P_{dr} &= V_{dr} I_d \quad \text{for current specification} \\
Q_{dr} &= P_{dr}\tan\phi_r \\
V_{di} &= V_{dr} - R_{dc} I_d \\
V_{doi} &= \frac{3\sqrt{2}}{\pi} B_i T_i E_{aci} \\
\gamma &= \cos^{-1}\left(\frac{V_{di} + R_{ci} B_i I_d}{V_{odi}}\right) \\
\phi_i &= \cos^{-1}(V_{di}/V_{doi}) \\
P_{di} &= V_{di} I_d \\
Q_{di} &= P_{di}\tan\phi_i
\end{aligned} \tag{4.40}$$

4.5.3 Incorporation of Control Variable Limits:

At each converter, the angle (α or γ) and the transformer tap (T) can be controlled directly to achieve (i) current control (ii) DC voltage control (iii) power control or (iv) control of reactive power. The control strategies of tap change control are explained in the following sections.

4.5.3.1 Rectifier and Inverter Transformers' Tap Adjustments in Mode-1

The tap changer control at the rectifier is designed to maintain the delay angle, α within the nominal range (say 10° to 20°) in order to achieve certain voltage margin for the purpose of current control. This has been implemented as follows:

1. If α violates the upper or lower limit of the nominal range, then T_r is adjusted as

$$T_{r(k+1)} = T_{r(k)} \pm \triangle T_r \tag{4.41}$$

where, $$\triangle T_r = \frac{(T_{rmax} - T_{rmin})}{N_r}$$
T_{rmax} = specified rectifier transformer upper limit.

T_{rmin} = specified rectifier transformer lower limit.
N_r = specified rectifier transformer number of tap positions.

2. If transformer tap-limits are reached, then the taps are set at the limiting values.

3. Compute V_{dor} and α.

When converters are operating in *Mode-1*, normally V_{di}^{sp} is specified. This specified value must correspond to the inverter tap setting which is within the specified range of tap positions. However, if V_{di}^{sp} specified leads to a tap setting out of the specified tap range, then the transformer tap is set at the limiting values and the V_{di}^{sp} is recomputed as per (4.42).

$$\begin{aligned} V_{doi} &= \frac{3\sqrt{2}}{\pi} B_i T_i E_{aci} \\ V_{di} &= V_{doi} \cos\gamma_{min} - R_{ci} B_i I_d \end{aligned} \tag{4.42}$$

The above procedures are depicted in Figure 4.6.

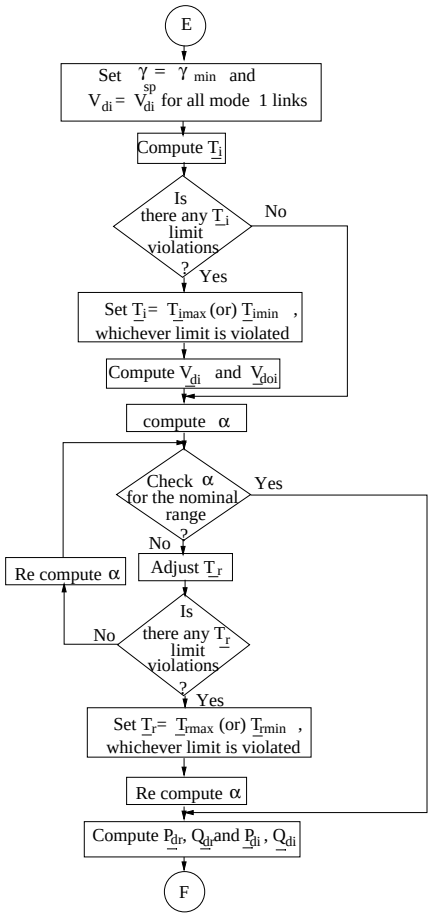

Figure 4.6: Flowchart for Mode-1 calculations.

4.5.3.2 Rectifier and Inverter Transformers' Tap Adjustments in Mode-2

In this mode, the rectifier transformer tap is adjusted to maximize DC voltage and the inverter transformer tap is adjusted so that $\gamma > \gamma_{min}$ and var consumption is minimized. In Figure 4.7, only inverter transformer tap-setting objective is met. The adjustment procedure is illustrated below.

1. If $\gamma < \gamma_{min}$ then adjust the T_i as follows:

$$T_{i(k+1)} = T_{i(k)} - \triangle T_i \tag{4.43}$$

where, $$\triangle T_i = \frac{(T_{imax} - T_{imin})}{N_i}$$

T_{imax} = specified inverter transformer upper limit.
T_{imin} = specified inverter transformer lower limit.
N_i = specified inverter transformer number of tap positions.

2. If transformer-tap-limits are reached, then the taps are set at the limiting values.

3. Compute γ and V_{doi}.

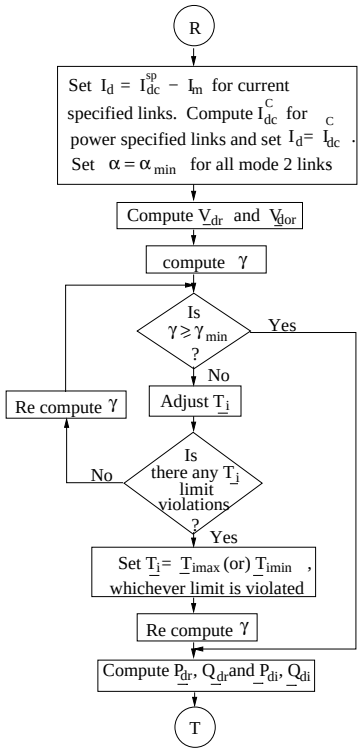

Figure 4.7: Flowchart for Mode-2 calculations.

NOTE: If $\gamma < \gamma_{min}$ at the limiting values of T_i, it may be required to re-adjust γ_{min} and/or T_{imax}/T_{imin} specifications.

4.5.4 AC-DC Load Flow Algorithm:

After obtaining the rectifier and inverter bus powers P_{dr}, Q_{dr}, P_{di} and Q_{di}, from (4.39) and (4.40), $\underline{P_{dc}}$ and $\underline{Q_{dc}}$ are calculated as

$$\underline{P_{dc}} = [\underline{P_{dr}}, -\underline{P_{di}}]^T \tag{4.44}$$

$$\underline{Q_{dc}} = [\underline{Q_{dr}}, \underline{Q_{di}}]^T. \tag{4.45}$$

Treating the above powers as fictitious loads, these quantities are interfaced with the existing AC load flow as:

$$\underline{P_L} = \underline{P_{Lo}} + \underline{P_{dc}} \tag{4.46}$$

$$\underline{Q_L} = \underline{Q_{Lo}} + \underline{Q_{dc}} \tag{4.47}$$

Where, $\underline{P_{Lo}}$ and $\underline{Q_{Lo}}$ represent the vector of nominal loads in the AC system.
NOTE:

1. The DC system filter admittances B_{sh} are considered as shunts and are accounted in a usual manner in the bus admittance matrix.

2. If voltage-dependent and/or frequency-dependent load modelling is to be considered, then $\underline{P_{Lo}}$ and $\underline{Q_{Lo}}$ are accordingly modified (see section 4.4).

These fictitious load powers are used to compute the bus power specifications $\underline{P}^{sp} = \underline{P}_G - \underline{P}_L$ and $\underline{Q}^{sp} = \underline{Q}_G - \underline{Q}_L$ in the AC routine (see Figure 4.5). If bus power mismatches are not below the prescribed tolerance value, i.e., if AC solutions are not converged, the AC load flow routine computes a new set of AC bus voltages and are used in the next DC calculations. The complete flowchart for the FDLF programme with the inclusion of HVDC links and load models is given in Figure 4.8. In the figure, the module 'AC Load Flow' represents the standard FDLF scheme (with a provision for inclusion of Q-limits at PV-buses using an index 'Q-bit' as discussed in section 4.3.2). A flag, 'DC-bit' facilitates the inclusion of DC links in the AC load flow.

A sample run for the IEEE 14-bus system with 2 two-terminal HVDC links and with the following specification (refer Table 4.6), is shown in section 5.2.

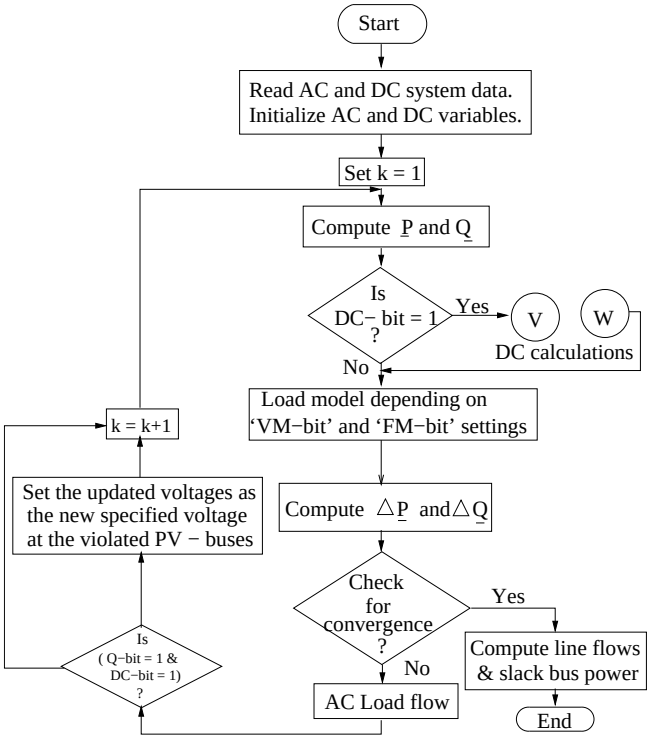

Figure 4.8: Flowchart for the inclusion of DC calculations in AC load flow.

Parameter	Link (5-4)		Link (1-2)	
	Rectifier	Inverter	Rectifier	Inverter
Bus No.	5	4	1	2
B	1	1	1	1
X_c	0.126	0.07275	0.1512	0.0873
$\alpha_{min}, \gamma_{min}$	5^o	15^o	5^o	15^o
T	$\pm 15\%$	$\pm 15\%$	$\pm 15\%$	$\pm 15\%$
N	27	19	25	20
T_n	1	1	1	1
B_{sh}	0.4902	0.6301	1.9608	1.0
R_{dc}	0.0034		0.0035	
P_{dr}^{sp}	0.5865		1.5858	
V_{di}^{sp}	1.284		1.237	
I_{dc}^{sp}	0.4562		1.2774	

Table 4.6: DC link data for the IEEE 14-bus system.

Chapter 5

Case Studies with A Test System: FDLF method

The single line diagram of the IEEE 14-bus system is shown in Figure 3.1. The system details are adopted from [13]. To run the load flow programme using FDLF method, the file required is: `fdlf_loadflow.m`. This file in turn calls the following `.m` files:

1. `B_bus_form.m`: It constructs B' and B'' matrices.
2. `fdlf_jacob_form.m`: It performs the solution of load flow equations till the solution is converged.
3. `dcflow.m`: It performs the mode checks and calculates bus powers at the HVDC link converter buses.
4. `dcdata.m`: It prepares the necessary data for the DC power flow using the input data files.
5. `powerflow.m`: It calculates the line flows and line losses.
6. `lfl_result.m`: It constructs the result files: `lfl.dat` and `report.dat`.

The above files require the following data files:

1. `busno.dat` : System details- number of lines, buses, transformers, etc.
2. `nt.dat` : Transmission line and transformer data.
3. `pvpq.dat` : Generation data and load data.
4. `shunt.dat` : Shunt data.
5. `Qlim_data.dat` : Reactive power generation limits data at PV-buses.

6. `load_model.dat` : Voltage-dependent load models data.

7. `freq_model.dat` : Frequency-dependent load models data.

8. `hvdc.dat` : DC link data -transformer taps, number of bridges per pole, α etc.

9. `spdata.dat` : DC link Specifications- current/power specification for each link.

On successful run, it generates three output files: `lfl.dat`, `report.dat` and `hvdc_res.dat`. The converged loadflow results are available in `lfl.dat`. The final converged DC link results are given in `hvdc_res.dat`.

5.1 Format of Data Files

In the following lines the format of each of the data file has been given using the IEEE 14-bus system data:
System details:

```
File name: busno.dat
------------------------------------------------------------------------
1       -----> Slack bus number.
0.001   -----> Loadflow convergence tolerance.
14      -----> Number of buses in the system.
17      -----> Number of lines. (existing ac lines are replaced by DC links)
3       -----> Number of transformers.
4       -----> Number of PV buses = (Number of generators - 1).
1       -----> To account Q-limits set this bit 1, otherwise 0. (Q-bit)
0       -----> To account volt-dep. loads set this bit 1, otherwise 0. (VM-bit)
0       -----> To account freq-dep. loads set this bit 1, otherwise 0. (FM-bit)
11      -----> Number of load buses (including loads at PV and slack buses).
1       -----> Number of shunts.
1.06    -----> Slack bus voltage magnitude.
0       -----> No of HVDC links (DC-bit).
------------------------------------------------------------------------
```

NOTE: The formats of files: `nt.dat`, `pvpq.dat`, `shunt.dat` , `lfl.dat` and `Qlim_data.dat` are identical to that given for NR-method -see section 3.2.1.

Voltage-dependent load models:

File name: load_model.dat

Load Bus No.	a1	a2	a3	b1	b2	b3
2	0.4	0.3	0.3	0.4	0.3	0.3
3	0.4	0.3	0.3	0.4	0.3	0.3
6	0.4	0.3	0.3	0.4	0.3	0.3
2	0.4	0.3	0.3	0.4	0.3	0.3
3	0.4	0.3	0.3	0.4	0.3	0.3
6	0.4	0.3	0.3	0.4	0.3	0.3
4	0.4	0.3	0.3	0.4	0.3	0.3
5	0.4	0.3	0.3	0.4	0.3	0.3
9	0.4	0.3	0.3	0.4	0.3	0.3
10	0.4	0.3	0.3	0.4	0.3	0.3
11	0.4	0.3	0.3	0.4	0.3	0.3
12	0.4	0.3	0.3	0.4	0.3	0.3
13	0.4	0.3	0.3	0.4	0.3	0.3
14	0.4	0.3	0.3	0.4	0.3	0.3

Frequency-dependent load models:

File name: freq_model.dat

```
0.1        ----> Frequency convergence factor (Cf).
2.0        ----> The frequency coefficient for real power (Kpf).
-1.5       ----> The frequency coefficient for reactive power (Kqf).
2.371545   ----> The real power generation at slack bus. P^{sp}_{Gs}
```

NOTE:

1. The `load_model.dat` is used if 'VM-bit'= 1. Constant power type load models are assumed if there are no entries for loads (both real and reactive power) at a load bus.

2. The `freq_model.dat` is used if 'FM-bit'= 1.

5.2 IEEE 14-bus Example for Inclusion of HVDC Link

In the original IEEE 14-bus system, two AC lines are replaced by HVDC links: one DC link between buses 5 and 4 (with I_{dc}^{sp} specification), and the second DC link between buses 1 and 2 (with P_{dr}^{sp} specification) -see Figure 5.1. In addition, Q-limits at PV-buses have been accounted. The DC link details (in pu.) are given in Table 4.6 (adopted from [28]). The base values used are: 100 MVA and 100 kV. See Appendix for base selection for DC system.

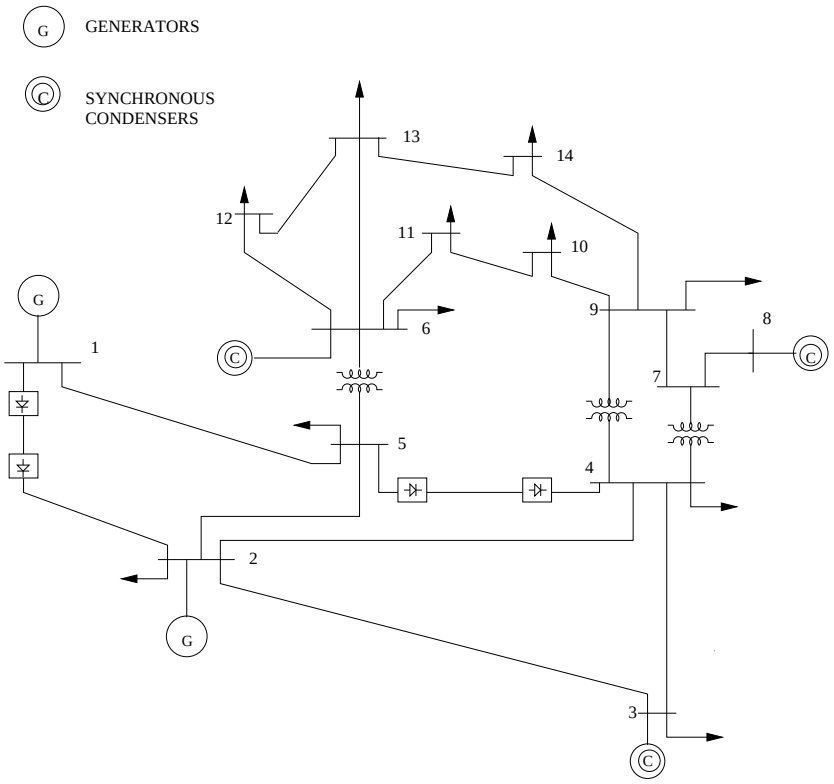

Figure 5.1: The modified IEEE 14-bus system.

The format of various input files pertaining to DC links is as follows:

HVDC Link data:

File name: hvdc.dat

Link No.	Rec/Inv bus	Br/Bi	Tr_max/Ti_max	Tr_min/Ti_min	Tn_r/Tn_i
1	5	1	1.15	0.85	1.0
1	4	1	1.15	0.85	1.0
2	1	1	1.15	0.85	1.0
2	2	1	1.15	0.85	1.0

Xcr/Xci	Alpha_min/Gama_min	Nr/Ni	Bshr/Bshi	
0.126	5	27	0.4902	----> link 1 Rectifier data
0.07275	15	19	0.6301	----> link 1 Inverter data
0.1512	5	25	1.9608	----> link 2 Rectifier data
0.0873	15	20	1.0	----> link 2 Inverter data

HVDC Link Specifications-related data:

File name: spdata.dat

Link No.	Rec-bus	Inv-bus	Vdis	Idc	Pdr	Im	Rdc
1	5	4	1.284	0.4562	0.5865	0.04	0.0034
2	1	2	1.237	1.2774	1.5858	0.12	0.0035

Alpha_min	Alpha_max	cn	pn	Vbase (kV)	Vdrs(initial)	
10	20	1	0	100	1	----->Link 1 specified data
10	20	0	1	100	1	----->Link 2 specified data

cn -set 1 if the dc link is on link current specification.

pn -set 1 if the dc link is on rectifier-end power specification.

For this case, where Q-limits are accounted, the files `busno.dat` and `nt.dat` are modified as follows:

File name: busno.dat

```
1       -----> Slack bus number.
0.001   -----> Loadflow convergence tolerance.
14      -----> Number of buses in the system.
15   *  -----> Number of lines. (existing ac lines are replaced by DC links)
3       -----> Number of transformers.
4       -----> Number of PV buses = (Number of generators - 1).
1       -----> To account Q-limits set this bit 1, otherwise 0. (Q-bit)
0       -----> To account volt-dep. loads set this bit 1, otherwise 0. (VM-bit)
0       -----> To account freq-dep. loads set this bit 1, otherwise 0. (FM-bit)
11      -----> Number of load buses (including loads at PV and slack buses).
1       -----> Number of shunts.
1.06    -----> Slack bus voltage magnitude.
2    *  -----> No of HVDC links (DC-bit).
```

* -indicates the changes made with respect to the original `busno.dat`.

Network data:

File name: nt.dat

From	To	R	X	y (total)/Tap ratio	Remarks
%1	2	0.01938	0.05917	0.0528	---> Line 1
1	5	0.05403	0.22304	0.0492	---> Line 2
2	3	0.04699	0.19797	0.0438	---> Line 3
2	4	0.05811	0.17632	0.034	---> Line 4
2	5	0.05695	0.17388	0.034	---> Line 5
3	4	0.06701	0.17103	0.0128	---> Line 6
%4	5	0.01335	0.04211	0.00	---> Line 7
7	8	0.0	0.17615	0.0	---> Line 8
7	9	0.0	0.11001	0.0	---> Line 9
9	10	0.03181	0.08450	0.0	---> Line 11
6	11	0.09498	0.19890	0.0	---> Line 11
6	12	0.12291	0.25581	0.0	---> Line 12

```
  6     13     0.06615   0.13027   0.0                      ---> Line 13
  9     14     0.12711   0.27038   0.0                      ---> Line 14
  10    11     0.08205   0.19207   0.0                      ---> Line 15
  12    13     0.22092   0.19988   0.0                      ---> Line 16
  13    14     0.17093   0.34802   0.0                      ---> Line 17
  4     7      0.0       0.20912   0.978 ---> Transformer data starts here.
  4     9      0.0       0.55618   0.969
  5     6      0.0       0.25202   0.932
--------------------------------------------------------------------------
```

NOTE:

Since two AC lines: 1-2 and 4-5 are replaced by two-terminal HVDC links, these two lines must be deleted from the file `nt.dat`. Instead, one may comment out these two rows as shown above.

With a tolerance factor, $\epsilon = 0.001$ and without considering load models, the solution has taken 4 P-iterations and 3 Q-iterations to reach convergence. The partial content of file `report.dat` is shown below.

```
~~~~~~~~~~~~~~~~~~~~~~~~~~~~~~~~~~~~~~~~~~~~~~~~~~~~~~~~~~~~~~~~~~~~~~~~~~~~~
 Loadflow results:
--------------------------------------------------------------------------
```

Bus No	VbO	thetaO	PGO	QGO	PLO	QLO
1	1.060000	0.000000	2.286187	-1.250493	0.000000	0.000000
2	1.047204	-4.081198	0.400000	-0.397088	0.217000	0.127000
3	1.010581	-11.736848	0.000000	0.000133	0.942000	0.190000
4	1.058625	-10.249079	0.000000	0.000000	0.478000	-0.039000
5	1.029111	-8.156934	0.000000	0.000000	0.076000	0.016000
6	1.070000	-13.530646	0.000000	0.018110	0.112000	0.075000
7	1.079937	-13.131210	0.000000	0.000000	0.000000	0.000000
8	1.090000	-13.131210	0.000000	0.062267	0.000000	0.000000
9	1.073443	-14.659714	0.000000	0.000000	0.295000	0.166000
10	1.065463	-14.750492	0.000000	0.000000	0.090000	0.058000
11	1.064285	-14.285811	0.000000	0.000000	0.035000	0.018000
12	1.056551	-14.401321	0.000000	0.000000	0.061000	0.016000
13	1.052942	-14.527435	0.000000	0.000000	0.135000	0.058000
14	1.046708	-15.585947	0.000000	0.000000	0.149000	0.050000

Line flows:

		Line flows				Line flows	
From	To	P-flow	Q-flow	From	To	P-flow	Q-flow
1	5	0.7004	-0.0010	5	1	-0.6768	0.0448
2	3	0.7284	0.0445	3	2	-0.7055	0.0058
2	4	0.6000	-0.2478	4	2	-0.5781	0.2765
2	5	0.4347	-0.0364	5	2	-0.4249	0.0297
3	4	-0.2365	-0.1956	4	3	0.2425	0.1973
7	8	0.0000	-0.0617	8	7	-0.0000	0.0623
7	9	0.2811	0.0675	9	7	-0.2811	-0.0596
9	10	0.0522	0.0817	10	9	-0.0520	-0.0810
6	11	0.0736	-0.0039	11	6	-0.0731	0.0048
6	12	0.0767	0.0199	12	6	-0.0760	-0.0185
6	13	0.1767	0.0517	13	6	-0.1747	-0.0478
9	14	0.0961	0.0615	14	9	-0.0947	-0.0585
10	11	-0.0381	0.0230	11	10	0.0382	-0.0227
12	13	0.0150	0.0025	13	12	-0.0150	-0.0025
13	14	0.0548	-0.0075	14	13	-0.0543	0.0085
4	7	0.2811	0.0200	7	4	-0.2811	-0.0058
4	9	0.1622	0.0437	9	4	-0.1622	-0.0305
5	6	0.4390	0.1704	6	5	-0.4390	-0.1246

Total real power losses in the system = 0.096122

Total reactive power losses in the system = -4.533410

NOTE:

The expressions used for the calculation of line flows and the system losses with HVDC links, are given in Appendix.

Results of The D.C.Link: 1

Parameter	Rectifier	Inverter
Bus no	5	4
D.C.Voltage(pu)	1.285551	1.284000
Transformer tap Position(pu)	1.011111	0.952757
Control Angles(Deg)	17.466154	15.000000
Commutation overlap Angles(Deg)	11.397456	8.162801
Real Power flow(pu)	0.586468	0.585761
Reactive power consumption(pu)	0.258883	0.207395
Power factor	0.914833	0.942658
Current in the D.C.Link(pu)	0.456200	

Voltage Base in kV = 100.00

Results of The D.C.Link: 2

Parameter	Rectifier	Inverter
Bus no	1	2
D.C.Voltage(pu)	1.241471	1.237000
Transformer tap Position(pu)	1.012000	0.983495
Control Angles(Deg)	10.173883	15.000000
Commutation overlap Angles(Deg)	32.968526	20.629222
Real Power flow(pu)	1.585800	1.580089
Reactive power consumption(pu)	0.953687	0.812281
Power factor	0.856966	0.889365
Current in the D.C.Link(pu)	1.277356	

Voltage Base in kV = 100.00

converged D.C Load flow Results:

File name: hvdc_res.dat

Rec/ Inv	Vdr/ Vdi	Tr/ Ti	Pdr/ Pdi	Qdr/ Qdi	Alpha/ Gama	P.f	Vbase
5	1.285551	1.011111	0.586468	0.258883	17.466154	0.914833	100.00
1	1.241471	1.012000	1.585800	0.953687	10.173883	0.856966	100.00
4	1.284000	0.952757	0.585761	0.207395	15.000000	0.942658	100.00
2	1.237000	0.983495	1.580089	0.812281	15.000000	0.889365	100.00

Appendix A

Important Expressions Used in Load Flow Programme

Computation of Line Flows

Transmission network mainly consists of transmission lines and transformers. The modelling of these components are briefly discussed in the following sections:

Transmission Lines:

Transmission Lines are modelled as a nominal π circuit [6] as shown in Figure A.1.

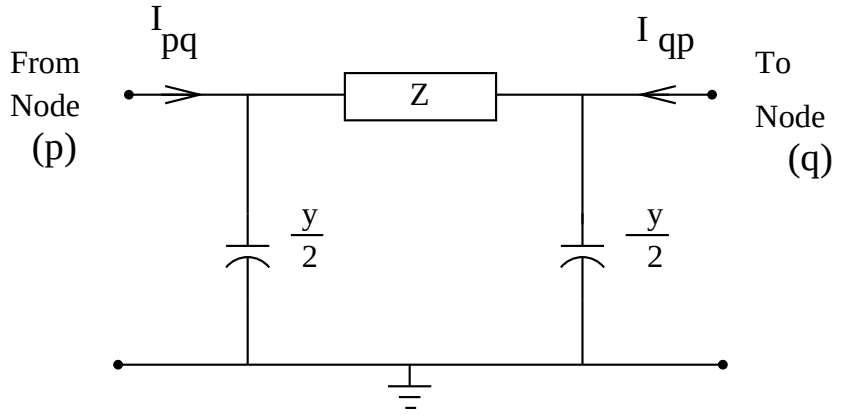

Figure A.1: Nominal π Model of transmission lines.

where,

Z: represents the series impedance of the line.

$\frac{y}{2}$: represents half of the total line charging y, at each node.

Transformers:

The transformers are generally used as inter-connecting (IC) transformers and generator transformers. These transformers are usually with off-nominal turns ratio and notations used are shown in Figure A.2. The π equivalent circuit [6] of transformer is given in Figure A.3.

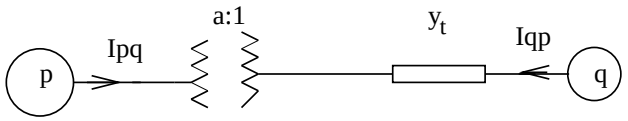

Figure A.2: Transformer with off-nominal tap.

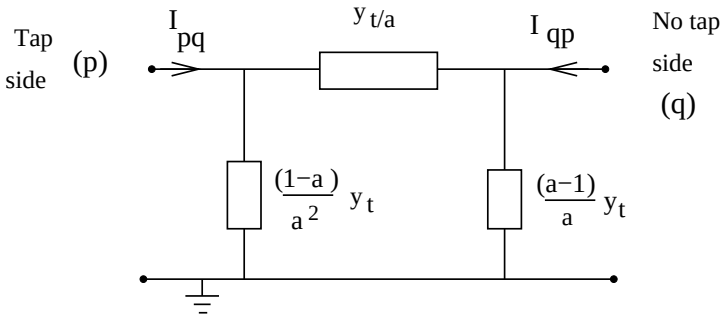

Figure A.3: Equivalent circuit of transformer.

where,

$y_t = \frac{1}{z_t}$

z_t: represents the series impedance at nominal-turns-ratio.

a: represents per unit off-nominal tap position.

1. For transmission lines: For the above model, the line currents I_{pq} and I_{qp} are computed as

$$\begin{aligned} I_{pq} &= \frac{(V_p - V_q)}{Z} + V_p \frac{y}{2} \\ I_{qp} &= \frac{(V_q - V_p)}{Z} + V_q \frac{y}{2} \end{aligned} \tag{A.1}$$

2. For transformers : In Figure A.3 assume that,

$$\begin{aligned} Y_1 &= \frac{y_t}{a} \\ Y_2 &= \frac{(1-a)}{a^2} y_t \\ Y_3 &= \frac{(a-1)}{a} y_t \end{aligned}$$

The currents I_{pq} and I_{qp} are computed as

$$\begin{aligned} I_{pq} &= (V_p - V_q)Y_1 + V_p Y_2 \\ I_{qp} &= (V_q - V_p)Y_1 + V_q Y_3 \end{aligned} \tag{A.2}$$

The complex apparent powers S_{pq} and S_{qp} are calculated as

$$\begin{aligned} S_{pq} &= P_{pq} + jQ_{pq} = V_p I_{pq}^* \\ S_{qp} &= P_{qp} + jQ_{qp} = V_q I_{qp}^* \end{aligned}$$

The net power loss in the component connected between nodes p and q is given by

$$S_{pq-loss} = S_{pq} + S_{qp}$$

If any shunt element ($Y_{shp} = G_p + jB_p$) is present at node p, the shunt current and hence the complex apparent power at node p are given by

$$\begin{aligned} I_{shp} &= V_p Y_{shp} \\ S_{shp} &= V_p I_{shp}^* \end{aligned}$$

The total apparent power loss in the system is given by

$$\begin{aligned} S_{loss} &= \sum_{all\ lines\ and\ transformers} S_{pq-loss} + \sum_{all\ shunts} S_{shp} = \sum_{all\ dc\ links} I_d^2 R_{dc} \\ &= \sum_{p=1}^{n} \left[P_{Gp} - P_{Lp}\right] + j\left[Q_{Gp} - (Q_{Lp} + Q_{dcp})\right] \end{aligned} \tag{A.3}$$

or in terms of bus power injection S_p at bus p, the S_{loss} is given by

$$S_{loss} = \sum_{p=1}^{n} S_p - (P_{Ls} + jQ_{Ls}) - (P_{dcs} + jQ_{dcs}) + \sum_{all\ dc\ links} I_d^2 R_{dc} \tag{A.4}$$

Computation of Overlap Angles:

The commutation overlap angles at rectifier and inverter bus are computed as,

$$\mu_r = cos^{-1}\left(2\frac{V_{dr}}{V_{dor}} - \cos\alpha\right) - \alpha \tag{A.5}$$

$$\mu_i = cos^{-1}\left(2\frac{V_{di}}{V_{doi}} - \cos\gamma\right) - \gamma \tag{A.6}$$

Base Selection for DC System

Base quantities for the DC system are chosen as follows:

$$\begin{aligned} S_B^{DC} &= S_B^{AC} \\ V_B^{DC} &= V_B^{AC} \\ I_B^{DC} &= \frac{S_B^{DC}}{V_B^{DC}} \\ Z_B^{DC} &= \frac{V_B^{DC}}{I_B^{DC}} \end{aligned} \tag{A.7}$$

MATLAB Implementation:

1. The linearized load flow equation given by (2.14) for N-R method, and $P-\delta$ and $Q-|V|$ equations given by (4.20) and (4.21), respectively, for FDLF method, are of the form $A\underline{x} = \underline{b}$. In MATLAB, the solution for the correction vector is obtained by using 'backslash' command as follows:

   $$\underline{x} = A\backslash\underline{b}$$

2. In the programming, all variables have been vectorized and declared as *sparse* to exploit the advantage of sparsity solution techniques which is inherent to MATLAB.

Bibliography

[1] IEEE Recommended practice for industrial and commercial power Systems Analysis.*IEEE Standards*, 399 -1997

[2] G.T.Heydt, *Computer Methods in Power System Analysis*, Macmillan Publishing Company, New York, 1986.

[3] Glenn W. Stagg and Ahmed H. El-Abiad, *Computer Methods in Power System Analysis*, McGraw-Hill Inc, New York, 1968.

[4] Elgerd O.I, *An Introduction Electric Energy Systems Theory*, Tata Mc Graw-Hill Publishing Company Limited, Bombay, 1983.

[5] Saadat. H, *Power System Analysis*, McGraw-Hill Publishers, Singapore, 1999.

[6] M.A. Pai, *Computer Techniques in Power System Analysis*, Tata McGraw-Hill Publishing Company Ltd, New Delhi, 1979.

[7] Stott B and O. Alsac, "Fast Decoupled Load Flow method", *IEEE Trans on Power Apparatus and Systems*, Vol.PAS-93, pp. 859-869, 1974.

[8] W.F. Tinny and C.E. Hart, "Power flow solution by Newton's method", *IEEE Trans. on Power Apparatus and Systems*, Vol.86, No. 8, pp. 1449-56, November, 1967.

[9] Show-kang Chang, and Vladimir Brandwajn, "Adjusted solutions in fast decoupled load flow", *IEEE Trans. on Power Systems*, Vol. 3, No. 2, pp. 726-733, May 1988.

[10] Stott. B, "Review of loadflow calculation methods", *Proceedings of the IEEE*, Vol.62, pp. 916-929, 1974.

[11] John J. Grainger and William D. Stevenson Jr, *Power System Analysis*, McGraw-Hill Inc, New York, 1994.

[12] P.Kundur, *Power System Stability and Contol*, McGraw-Hill Inc, New York, 1994.

[13] Power system test cases archive, UWEE, *www.ee.washington.edu/research/pstca*.

[14] IEEE committe report "Transient stability test systems for direct stability methods", *IEEE Trans on power systems* Vol.7, pp. 37-43, Feb., 1992.

[15] *Using MATLAB*, Version 5.3, Release 11, The Math Works Inc.

[16] Robert A.M. Van Amerongen, "A general-purpose version of the Fast Decoupled Load flow", *IEEE Trans. on Power Systems*, Vol. 4,No.2, pp. 760-770, May, 1989.

[17] Hubbi,W., "Effects of of neglecting resistances in XB and BX load flow methods", *IEE Proceedings*, Vol.C, No.138, pp. 452-456, 1991.

[18] S.A Soman, S.A Khaparde and Shubha Pandit, *Computational Methods for Large Sparse Power Systems Analysis: An Object Oriented Approach*, Kluwer Academic Publishers., Boston/London, 2002.

[19] Kusic G.L, *Computer Aided Power System Analysis*, Prentice, New Delhi, 1989.

[20] K.R. Padiyar, *Power System Dynamics - Stability and Control*, BS Publications, Hyderabad, India, 2002.

[21] P S R Murty, "Load modelling for power flow solutions", *J Inst Eng (India) Electr.Eng Div.*, 58 pt EL3., pp. 162-165, December 1977.

[22] IEEE Committee Report,"Standard load models for power flow and dynamic performance simulations *IEEE Trans. on Power Systems*, Vol. 10, No. 3, pp. 1302-1313, August, 1995.

[23] Kimbark,E.W, *Direct Current Transmission* , Vol. 1, Wiley Limited, New york, 1971.

[24] K.R.Padiyar, *HVDC Power Transmission Systems Technology and System Interactions*, Wiley Eastern Limited, New Delhi, 1990.

[25] Dusan Povh, Fellow, IEEE, "Use of HVDC and FACTS", *Proceedings of the IEEE.*, Vol. 88, No. 2, February 2000.

[26] T.J. Hammons, D. Woodford, J. Loughtan, M. Chamia, J. Donahoe, D. Povh, B. Bisewski, and W. Imng, "Role of HVDC transmission in future energy development", *IEEE Power Engineering Review*, pp. 10-25, February, 2000.

[27] Willis Long and Stig Nilson, "HVDC transmission: yesterday and today", *IEEE Power & Energy System magazine (Special issue on HVDC systems (pp. 32-61))*, Vol.5, No.2, pp. 22-31, march/ April 2007.

[28] Arrillaga.J, and Arnold C.P, *Computer Analysis of Power Systems*, John Wiley Limited, New Delhi, 1990.

Acknowledgments

The authors thank Prof. A.M.Kulkarni at IIT Bombay for his valuable suggestions and discussions regarding the programme implementation.

Please report bugs to: *knsa1234@yahoo.com* or *knsa@nitk.ac.in*